

**Widespread Infection of the Hair Lichen Genus *Bryoria* (Parmeliaceae) by a
Previously Unknown Fungal Pathogen**

by

Spencer James Goyette

A thesis submitted in partial fulfillment of the requirements for the degree of

Master of Science

Department of Biological Sciences
University of Alberta

© Spencer James Goyette, 2020

ABSTRACT

Bryoria Brodo & D. Hawksw. (Parmeliaceae, Ascomycota) is one of the dominant genera of hair lichens in western North America and is characteristic of high elevation conifer forest ecosystems. In areas where *Bryoria* is abundant, it is common to find thalli in which the thalline filaments become conglutinated, forming brittle dead zones, or “rattails”. I sampled *Bryoria* thalli across western Canada and the northwestern United States monitoring thallus dieback at different times of the year. I found that this dieback phenomenon is associated with the winter growth of a mold-forming basidiomycete not previously known to associate with *Bryoria*. Similar *Bryoria* die-off has been attributed to extreme rain events in British Columbia and Norway, but not in the presence of a necrotrophic mold. I report that this fungus belongs to *Athelia* Pers., a cosmopolitan genus of the basidiomycete family Atheliaceae containing economically significant pathogens. To place the *Bryoria*-associated fungi within *Athelia*, I designed *Athelia*-specific primers for two gene regions (EF1- α and ITS) and screened the mold directly along with apparently uninfected lichen specimens to assess its potential latent occurrence. The pathogen initially appeared to be related to *A. epiphylla* Pers. and *A. acrospora* Jülich, a species heretofore known only from dead wood. Based on phylogenetic placement along with its distinctly sized basidia and basidiospores, this mold is presented here as *Athelia seborrheica*, a new species. It was found to frequently infect members of *Bryoria* sect. *Implexae* (Gyeln.) Brodo & D. Hawksw., occasionally associates with other foliose and fruticose species within Parmeliaceae, and does not appear to exist within thalli asymptotically. Whether or not this widespread infection of *Bryoria* in western North America is a recent event or simply an overlooked

phenomenon is difficult to determine with certainty. This research will serve as a benchmark for documenting the pathogenic outbreak affecting an ecologically significant lichen genus.

PREFACE

This thesis is an original work by Spencer Goyette. Toby Spribille advised the methodology and approach, and Viacheslav Spirin (University of Helsinki) provided crucial specimens of *Athelia* as well as insight regarding that genus.

DEDICATION

But when you tread on this clutch of nettles
that was once me, reading this in some other century
like an outdated story, remember that I was innocent
and that like you, mortals of your day, I too
had a face marked by anger, and by pity, and by joy.

A man's face, quite simply.

Benjamin Fondane, "Préface en Prose", translated by John Balaban

One must have a mind of winter
To regard the frost and the boughs
Of the pine-trees crusted with snow;

And have been cold a long time
To behold the junipers shagged with ice,
The spruces rough in the distant glitter

Of the January sun; and not to think
Of any misery in the sound of the wind,
In the sound of a few leaves,

Which is the sound of the land
Full of the same wind
That is blowing in the same bare place

For the listener, who listens in the snow
And, nothing himself, beholds
Nothing that is not there and the nothing that is.

Wallace Stevens, "The Snow Man"

ACKNOWLEDGEMENTS

This work could not have been completed without the efforts, discussion, guidance, and support of many people. First and foremost I would like to thank my supervisor, Toby Spribille, for enlightening me to the ways of lichen-ness and for his guidance on everything during this whole process. Your ability to find decent lattes in the far-flung reaches of western North America is uncanny, and your knowledge of lichens is profound.

I would like to thank Justine Karst for her consistency, pragmatism, and supreme level-headedness during each of my committee meetings. I really benefitted from your support over the past two and a half years.

I want to thank Ross Evashkevich, my field assistant, for his help with collections throughout 2019 and his patience when plans needed to be changed last minute.

Thank you Trevor Goward, Göran Thor, Curtis Björk, Yngvar Gauslaa, and Darwyn Coxson for your life's work and inspirational discussions we've had in regards to lichen biology and hair lichen health.

I would also like to thank my labmates Veera Tuovinen, Gulnara Tagirdzhanova, Amelia Deneka, Carmen Allen, and David Díaz Escandón for putting up with me and for all the helpful talks we've had in our office, both big and small. I would like to additionally thank David Díaz Escandón and Andrew Cook for their help navigating different analyses in R.

Also, thank you Antonia Musso, Andrew Cook, and Monica Ayala Díaz for letting me hang with your pets.

And, ultimately, thanks to Karen Golinski for nudging me north and starting this whole endeavour.

This research was supported with start up funds from the Department of Biological Sciences at the University of Alberta granted to Toby Spribille and by the Alberta Conservation Association through the ACA Grants in Biodiversity Program.

TABLE OF CONTENTS

List of Tables	viii
List of Figures	ix
List of Plates	x
1 Introduction.....	1
2 Materials and Methods.....	3
3 Results.....	10
4 Discussion	14
5 Conclusion	20
6 Taxonomy	20
7 Tables, Figures, and Plates.....	25
References.....	88

LIST OF TABLES

Table 1: Voucher information for <i>Athelia</i> collected and sequenced for this study.....	25
Table 2: Voucher Information for Atheliaceae ITS and EF1- α sequences pulled from GenBank	39
Table 3: List of primers used and developed in this study to target <i>Athelia</i> (ITS and EF1- α) and <i>Bryoria</i> (ITS, IGS, and GAPDH) loci	40
Table 4: Voucher information for GenBank <i>Bryoria</i> sect. <i>Implexae</i> ITS, IGS, and GAPDH sequences from GenBank.....	41
Table 5: Results of the <i>Athelia</i> gene partitioning scheme and model selection indicate that ITS and each codon of EF1- α should run with separate evolutionary models during the maximum likelihood tree search	47
Table 6: Results of the <i>Bryoria</i> section <i>Implexae</i> gene partitioning scheme and model selection show that ITS, IGS, and each codon of GAPDH should run with separate evolutionary models during the maximum likelihood tree search.....	48
Table 7: Approximately Unbiased topology test results. Constraints of substrate preference do not explain evolutionary relationships across <i>Athelia</i>	49
Table 8: Average nucleotide pairwise distance results for <i>Athelia</i> ITS show greater nucleotide variation across members of <i>Athelia</i> than within <i>Athelia seborrheica</i>	50
Table 9: Average nucleotide pairwise distance results for <i>Athelia</i> EF1- α show greater nucleotide variation across members of <i>Athelia</i> than within <i>Athelia seborrheica</i>	51
Table 10: Results from the one-way analysis of variance (ANOVA) morphological measurements different <i>Athelia</i>	52
Table 11: Identity and frequency count of lichen hosts infected by <i>Athelia</i>	53
Table 12: Voucher information for <i>Bryoria</i> section <i>Implexae</i> collected and sequenced for this study	54
Table 13: Chemical and morphological data matrix for <i>Bryoria</i> section <i>Implexae</i> used in this study. No chemical or morphological species variant appear as preferential hosts of <i>Athelia</i>	59
Table 14: Diagnostic characters for <i>A. seborrheica</i> and similar species of <i>Athelia</i>	63

LIST OF FIGURES

Figure 1: Map of <i>Athelia</i> collections from this study	64
Figure 2: Constrained <i>Athelia</i> tree 1: <i>Athelia</i> from epiphytic lichen are monophyletic ..	65
Figure 3: Constrained <i>Athelia</i> tree 2: <i>Athelia</i> from fallen lichen are monophyletic.....	66
Figure 4: Constrained <i>Athelia</i> tree 3: <i>Athelia</i> from wood are monophyletic.....	67
Figure 5: Concatenated maximum likelihood tree of <i>Athelia</i> ITS and EF1- α color-coded by substrate preference per specimen isolate and whether basidioma measurements were taken. A new lineage of <i>Athelia</i> is supported	68
Figure 6: <i>Athelia</i> ITS maximum likelihood tree color-coded by substrate preference per specimen isolate and whether basidioma measurements were taken.....	70
Figure 7: <i>Athelia</i> EF1- α maximum likelihood tree color-coded by substrate preference per specimen isolate and whether basidioma measurements were taken	72
Figure 8: Box and whisker plot of <i>Athelia</i> basidioma measurements per species or species group show significant differences for <i>Athelia seborrheica</i> in basidium width and length, spore width, and sterigma length	73
Figure 9: Box and whisker plot of <i>Athelia</i> basidioma measurements per specimen color-coded by species or species group.....	75
Figure 10: Morphological differences between <i>Athelia</i> species or species groups displayed on a non-metric multidimensional scaling plot. There is almost complete overlap of all species on the basis of basidioma measurements	77
Figure 11: Concatenated maximum likelihood tree of <i>Bryoria</i> section <i>Implexae</i> ITS, IGS, and GAPDH color-coded to display which specimens hosted <i>Athelia</i> . There was no pattern explaining whether certain host species or species groups were preferentially infected.....	78

LIST OF PLATES

Plate 1: Healthy <i>Bryoria</i> sp.	81
Plate 2: <i>Bryoria</i> sp. with rattail	82
Plate 3: <i>Bryoria</i> sp. with visible fungal infection	83
Plate 4: Scanning Electron Microscope (SEM) micrograph of a healthy and infected <i>Bryoria</i> thallus with detailed features of the mold.....	84
Plate 5: <i>Athelia</i> on a fallen lichen covered branch, emerging just after snowmelt	86
Plate 6: Micro- and macroscopic images of basidioma from the <i>Athelia seborrheica</i> sp. nov. type specimen.....	87

CHAPTER 1

Widespread Infection of the Hair Lichen Genus *Bryoria* (Parmeliaceae) by a Previously Unknown Fungal Pathogen

1 INTRODUCTION

Sensitive to pollution and disturbance, the presence of lichens within a given habitat can be a useful indication of that habitat's health, age, and productivity (McCune, 2000). In boreal and montane forests, epiphytic lichens, such as those belonging to the genus *Bryoria* Brodo & D. Hawksw. (Parmeliaceae), interact with other organisms in a variety of ways. They serve as a crucial winter food source to sustain herds of critically endangered woodland caribou (Edwards et al., 1960; Rominger et al., 1996; Thomas et al., 1996; Johnson et al., 2000) and other ungulates (Ward & Marcum, 2010), are used as nesting material by flying squirrels (Maser et al., 1986) and birds (Pettersson et al., 1995), and can harbor diverse communities of invertebrates (Stubbs, 1989; Bokhorst et al., 2015). *Bryoria* and other hair lichens also contribute to epiphytic biomass in boreal forests (Campbell & Coxson, 2001) where their eventual decomposition is important to forest nutrient cycling (Pike, 1978; Coxson & Curteanu, 2002). Therefore understanding the health of *Bryoria* is central for understanding the health of the organisms with which they are linked.

Assessing the health of hair lichens can be a difficult task owing to the fact that lichens arise as a result of interactions between many disparate lineages of essentially microbial life forms (Ahmadjian, 1993; Spribille et al., 2020). Potentially pathogenic fungi have been isolated from healthy lichens (Petrini et al., 1990), but whether this could be the case for *Bryoria* remains to be thoroughly investigated. The presence of lichen-associated, or "lichenicolous", fungi (Hawksworth, 1983; Jeffries & Young, 1994; Lawrey & Diederich, 2003) has been used to

measure the health of a given lichen (Hawksworth, 1977; Gilbert, 1988). This is because lichenicolous fungi can produce discolorations, lesions, or dead areas on their lichen hosts (Lawrey & Diederich, 2003). However, beyond floristic or taxonomic studies, this group of fungi has not received much attention historically, and consequently much of their biology is still unknown. Interactions between the most pathogenic, or necrotrophic, lichenicolous fungi and their lichen hosts remain the best understood because they produce visible necroses on their hosts and kill them outright (Jülich, 1972; Hawksworth, 1977; Jülich & Stalpers, 1980; Jeffries & Young, 1994; Yurchenko & Golubkov, 2003). Other lichenicolous fungi exist in a commensal or "parasymbiotic" state (Lawrey & Diederich, 2003) where they can be visibly present on the host body, or "thallus", but are not associated with prominent discolourations or lesions (Rambold & Triebel, 1992).

Typical, healthy *Bryoria* thalli are free-flowing and knotless (Plate 1). However, in many *Bryoria* populations, it is common to find thalli clumping together and forming brittle dead zones, or "rattails", especially near the terminal ends of thalli (Plate 2). Mass dieback of *Bryoria* has been previously reported and found to be associated with unusually heavy and prolonged rain events in conifer forests in Norway and British Columbia (Goward 1998; Gauslaa 2002, 2014). These previous reports on *Bryoria* provide important connections between the ecophysiology of hair lichens with their health and were fundamental to the progress of this project. During the course of this study I found *Bryoria* rattails in all seasons, and in winter months these rattails were associated with an apparently cold-tolerant mold discovered by Toby Spribille in January 2019 in British Columbia (Plates 3 & 4). This contrasts with the Norwegian die-back event, in which no pathogenic mycelia were detected on *Bryoria* thalli (Gauslaa, 2002). Whether *Bryoria*

die-back events are commonplace and whether such events are driven by pathogens, physiological processes, or some combination of both is unknown.

In my thesis, I focus on investigating the role pathogens play in *Bryoria* dieback in western Canada. Specifically, the objectives for this study are to 1) identify the lichen pathogen or pathogens associated with the formation of *Bryoria* rattails, 2) determine whether the infection shows any patterns of lichen-host preference, and 3) assess whether the pathogen could exist as a cryptic, asymptomatic fungal symbiont, such has been recently reported for other lichens (Spribille et al., 2016; Tuovinen et al. 2019).

2 MATERIALS AND METHODS

2.1 Field collection

To collect material representing healthy and unhealthy hair lichens, and other potentially infected macrolichens, I surveyed boreal and montane conifer forests for *Bryoria* in western Canada and the northwestern United States. Hair lichen visibly infected with mold were collected in British Columbia, Alberta, Saskatchewan (Canada), Montana, and Idaho (USA) between 2019 and 2020 (Table 1, Fig. 1). Surveys were conducted from a range of elevations, from 130 meters to 1935 meters above sea level (Table 1, Fig. 1). Conifer trees in the genera *Picea*, *Abies*, and *Pseudotsuga* were the typical phorophytes of *Bryoria* collections. To determine whether the pathogen was present in Europe, additional collections were made by Toby Spribille in Sweden and Austria during the summer of 2019 (Table 1, Fig. 1). Only epiphytic lichens that were within standing reach (approximately 1 - 2.7 m) were collected. The upper canopy was never accessed for sampling. Infected lichens were categorized in two ways: as either material which had fallen to the ground (Plate 5) or material which was still epiphytic.

Owing to the ecological differences between soil surface and above-ground environments, I hypothesize that different fungal species would infect epiphytic versus fallen lichen material. Material that had fallen to the ground was collected opportunistically. Collection sites were selected by utilizing BING Maps (www.bing.com/maps). A map of all collections from this study (Fig. 1) was made using QGIS v2.18 (QGIS.org) with a WAD-84 coordinate reference system and the North Pole Lambert Azimuthal Equal Distance projection.

2.2 DNA extraction and sequencing - Pathogen

To identify the pathogen causing rattails in *Bryoria*, I extracted, amplified, and sequenced its DNA. Hyphae or, when present, basidiome tissue from the mold was separated from lichen-host material using an Olympus SZX16 dissecting scope prior to DNA extraction. Extractions were performed using the DNeasy Plant Mini Kit (QIAGEN, Hilden, Germany) per the manufacturer's instructions. Special attention was paid to reduce the amount of host tissue included in each extraction as excess lichen material gummed up the spin columns.

As host tissue could not be completely separated from the mold, I designed pathogen-specific markers for two loci – the internal transcribed spacer region (ITS) and the translation elongation factor 1- α (EF1- α) (Table 2). I chose these two loci because ITS is a commonly sequenced gene region for fungi (Schoch et al., 2012) and EF1- α is a variable gene region that has been shown to be informative when constructing molecular phylogenies (Roger et al., 1999). In addition, comparable sequence data for EF1- α were available via GenBank. These primers were designed by initially performing PCR with more general fungal ITS (White et al., 1990; Gardes & Bruns, 1993) and EF1- α primers (Rehner & Buckley, 2005), then extracting all positive bands from the electrophoresis gel with the QIAquick Gel Extraction Kit (QIAGEN,

Hilden, Germany) to be sequenced. To ensure that the primers did not amplify other fungal DNA known to be present in hair lichens, I aligned the resulting sequence fragments of the pathogen against publicly available sequences of the host mycobiont, as well as *Cyphobasidium* and *Tremella*, two basidiomycete yeasts known to be asymptotically present in lichen thalli (Spribille et al., 2016; Tuovinen et al., 2019) using AliView (Larsson, 2014). I used the ThermoFisher Oligo Design Tools web portal (ThermoFisher Scientific, Walten, Massachusetts, USA) to look for nucleotide motifs that discriminate against these other fungal sequences, and to ensure that the primers were chemically usable; specifically, that the primers contained roughly 40-60% GC, melting temperature was not too high, and primers were not self-binding. As a positive control, I re-ran PCRs with these primers using the DNA extractions from which they were initially sequenced. If a single band was produced I submitted the PCR product for sequencing (see below), and used the primers on new DNA extractions of the lichen pathogen.

Five μL dilutions of DNA extract were used in a twenty-two μL reaction with KAPA3G Plant PCR Kit (Millipore Sigma, Burlington, Massachusetts, USA) using the manufacturer's specifications and were run on a Veriti 96-Well Fast Thermal Cycler (Applied Biosystems, Foster City, California, USA) with the following programs for ITS: an initial denaturation at 95°C for 5 minutes, followed by 35 cycles of 95°C for 30 s, 57°C for 30 s, 72°C for 30 s, and a final extension of 72°C for 7 min; and for EF1- α : an initial denaturation at 95°C for 5 min, then nine touchdown cycles of 95°C for 1 min, 66-57°C for 30 s, 72°C for 1 min, then 36 cycles of 95°C for 30 s, 56°C for 30 s, 72°C for 1 min, and a final extension of 72°C for 10 min. Two μL aliquots of PCR product were viewed on 0.8% agarose gels stained with GelRed™ (Biotium, VWR, Hayward, California, USA). All positive bands were enzymatically purified using Exonuclease I and Shrimp Alkaline Phosphatase (New England BioLabs, Inc., Ipswich,

Massachusetts, USA). Sanger sequencing of all PCR products was outsourced to Psomagen (Rockville, Maryland, USA). Initial querying of the sequences against the NCBI nucleotide database using BLAST (Altschul et al., 1990) returned high-scoring hits from the basidiomycete genus *Athelia* Pers. (Atheliaceae). Viacheslav Spirin (University of Helsinki) provided *Athelia* material from collections he made across Eurasia and western North America (Table 1) for me to compare my sequences and specimens against. For this material, only basidiomata tissue was used for DNA extraction using the QIAamp DNA Investigator Kit (QIAGEN, Hilden, Germany). Successful sequence fragments from Psomagen were retrieved electronically, checked for electropherogram ambiguities with BioEdit (Hall, 1999), and subjected to a BLAST (Altschul et al., 1990) search to determine whether their approximate taxonomic grouping was different from the host-lichen identity.

2.3 Morphological analyses of pathogen

In addition to DNA analysis, morphological features were also used to identify the mold. Twenty-two specimens of *Athelia* producing basidiomata (Table 1), sexual structures of basidiomycetes, were included in this study. Fifteen measurements of basidium length, basidium width, sterigma length, sterigma width, basidiospore length, basidiospore width, and hyphal diameter were taken from each specimen. Basidioma squashes were viewed at 1000x on a Zeiss AXIO A.1 microscope and stained with 1% Phloxine-B in 5% potassium hydroxide (KOH), and rehydrated with water as necessary. Microscopic images were taken using an Olympus SC180 Color Camera and all measurements were made using Olympus cellSens software. A one-way analysis of variance (ANOVA) and subsequent Tukey's Honestly Significant Difference post-hoc test (Tukey HSD) were performed on these measurements in R v3.6.1 in RStudio v1.1.463 (R

Core Team, 2019) against mold species identity or species group as determined *a posteriori* to the generation of a phylogenetic tree (see *Phylogenetic analyses*). Multivariate analyses using all specimen measurements were performed with non-metric multidimensional scaling (NMDS) in the R package *vegan* v2.5-6 (Oksanen et al., 2019).

2.4 Host preference and identity

Often numerous species of lichen grow within close proximity to one another so I tested the preference of the rattail pathogen for particular lichen hosts. For this study, each macrolichen found to be visibly infected was identified to species or genus level using morphological and chemical characters (Brodo & Hawksworth, 1977; Goward et al., 1994; Goward, 1999; Myllys et al. 2011). In order to determine the identity of diagnostic secondary metabolites present within the host lichens, I performed chemical spot tests with potassium hydroxide, sodium hypochlorite, and *para*-phenylenediamine along with thin layer chromatography (TLC) in solvent solutions A and B according to Orange et al. (2001). The identification to species level of one group of lichen hosts, *Bryoria* sect. *Implexae* (Gyeln.) Brodo & D. Hawksw., is quite difficult using morphological characteristics or chemical techniques. Accordingly, DNA extractions of uninfected tissue for lichens within this group were amplified using markers for ITS, the intergenomic spacer (IGS), and glyceraldehyde-3-phosphate dehydrogenase (GAPDH), following a previous study on this group by Velmala et al. (2014) (Tables 3 & 4). Extractions were performed using the DNeasy Plant Mini Kit (QIAGEN) as per the manufacturer's instructions. Subsequently, five μ L dilutions of DNA extract were used in a twenty-two μ L PCR reaction with KAPA polymerase (Millipore Sigma) and run on a Veriti 96-Well Fast Thermal Cycler (Applied Biosystems) using the following programs for ITS: an initial denaturation at

95°C for 5 min, followed by 35 cycles of 95°C for 30 s, 57°C for 30 s, 72°C for 30 s, and a final extension of 72°C for 7 min; IGS: initial denaturation at 95°C, followed by 35 cycles of 95°C for 30 s, 55°C for 30 s, 72°C for 1 min, and a final extension of 72°C for 7 min; GAPDH: an initial denaturation at 95°C for 5 min, then 5 cycles of 95°C for 30 s, 56°C for 30 s, 72°C for 1 min, then 30 cycles of 95°C for 30 s, 54°C for 30 s, 72°C for 1 min, and a final extension of 72°C for 10 min (Velmalala et al., 2014). From each reaction, two μ L aliquots of PCR product were viewed on 0.8% agarose gels stained with GelRed™ (Biotium, VWR). All positive bands were enzymatically purified using Exonuclease I and Shrimp Alkaline Phosphatase (New England BioLabs, Inc.). Sanger sequencing of all PCR products was outsourced to Psomagen (Rockville, Maryland, USA). The electropherograms of successfully sequenced fragments were viewed on BioEdit (Hall, 1999) and subjected to initial BLAST (Altschul et al., 1990) analysis as mentioned above.

2.5 Latent symbiosis assessment

To test whether the fungal pathogen was present in apparently uninfected asymptomatic *Bryoria*, the pathogen-specific primers (Table 3) were used on 55 DNA extractions from healthy lichen material. I collected these healthy lichens in 2018, prior to the detection of the lichen mold. DNA extractions of six rattailed and visibly infected *Bryoria* specimens were included as positive controls.

2.6 Phylogenetic analyses

To delimit species identity of the mold and *Bryoria* sect. *Implexae* hosts, I constructed phylogenetic trees using a maximum likelihood (ML) approach. Sequences from the mold and *Bryoria* sect. *Implexae* were handled separately, but followed the same general protocol.

Each set of sequences were aligned with MAFFT v7 (Katoh & Standley, 2013), concatenated, and trimmed using custom python scripts developed by Resl (2015) and were implemented following Resl et al. (2015). The resulting alignments were manually edited using AliView (Larsson, 2014). Nucleotide substitution models were determined for each locus using PartitionFinder v2.1.1 (Lanfear et al., 2016). For the protein-coding genes (EF1- α and GAPDH), substitution models were determined individually for the first, second, and third codon positions (Tables 5 & 6). Maximum likelihood analysis was performed in IQ-TREE v2.0 (Nguyen et al., 2015). Branch supports were obtained with ultrafast bootstrapping (Hoang et al., 2018) of 1000 replicates. Only the branches which received ultrafast bootstrap values $\geq 95\%$ were considered well supported (Nguyen et al., 2015). Calculations for the number of variable and parsimonious sites as well as nucleotide composition were generated by IQ-TREE v2.0 (Nguyen et al., 2015). The resulting consensus tree topology was subjected to an Approximately Unbiased (AU) Test (Shimodaira, 2002) in IQ-TREE v2.0 with 1000 bootstrap replicates to evaluate possible alternative topologies based around substrate use (Figs. 2-4). Phylogenetic trees were visualized using FigTree v1.4.3 (Rambaut, 2014).

I also generated haplotype networks for the fungal pathogen to investigate patterns of genetic variation among the pathogen sequences in order to help with species delimitation. After I discarded sequences with ambiguous bases from each alignment, I generated haplotype networks from ITS and EF1- α using the R package *pegas* v0.12 (Paradis, 2010). Subsequently, the average pairwise nucleotide differences among sequence samples (Nei & Kumar, 2000)

within and between haplotype groups was calculated via the "nucleotideDivergence" function in the R package *strataG* v2.4.905 (Archer et al., 2016).

3 RESULTS

3.1 Pathogen identity and substrate preference

Based on morphology and phylogenetic analysis, the pathogen associated with the formation of rattails appeared to belong to the genus *Athelia*. A total of 98 new sequences of *Athelia* were produced for this study, including 66 ITS sequences and 32 EF1- α sequences (Table 1). The final concatenated alignment consisted of 1738 characters (ITS: 685; EF1- α : 1053), with 734 variable and 369 parsimony informative sites (Fig. 5). Based on AICc score and returned log likelihood values, each individual codon position for ITS and EF1- α ran with separate evolutionary models (Table 5). The topologies of each gene tree (Figs. 6 & 7) and the concatenated tree (Fig. 5) support a lineage of lichen-associated pathogens in *Athelia*, which includes all epiphytic material collected in North America for this study – except isolates SG357 and SG414 (see below) – as well as one European isolate from Sweden (SG624). This lineage was recovered as distinct from another known lichen pathogen, *Athelia arachnoidea* (Berk.) Jülich (Jülich, 1972; Jülich & Stalpers, 1980). One Albertan specimen from fallen, infected lichen material (SG639) was recovered as sister to *A. arachnoidea* in both the concatenated and ITS trees (Figs. 5 & 6). Several isolates from fallen lichen material (SG520, SG519, SG555, SG570, and SG573) and two from epiphytic lichens (SG357 and SG414) group with *A. acrospora* Jülich though this lineage was not phylogenetically well supported (Fig. 5).

Additionally, several species of *Athelia*, as identified on collection packets or previous accessions, were not recovered as monophyletic in any gene tree: *A. epiphylla* Pers., *A. decipiens*

(Höhn. & Litsch.) J. Erikss., *A. bombacina* Pers., and *A. cystidiolophora* Parm. (Figs. 5-7).

Individuals identified as *A. cystidiolophora* fail to form a well supported clade but appear with named sequences of *A. decipiens* and *A. epiphylla* (Figs. 5 & 6). Morphologically, *A. cystidiolophora* is quite distinct from other *Athelia* since it is one of two species which produce cystidia – diagnostic hyphal projections present in many basidiomycetes (Jülich, 1972; Jülich & Stalpers, 1980). Sequences from previously identified specimens of these four species were organized into two poorly supported species groups: Group I consisted of sequences from *A. decipiens*, *A. epiphylla*, and *A. cystidiolophora*; and, Group II with *A. bombacina* and *A. epiphylla* (Fig. 5). The position of one sample from fallen lichen material (SG518) was found as sister to Group I – *A. epiphylla* material in the EF1- α tree with 100% ultrafast bootstrap support (Fig. 7), unsupported but within Group I in the concatenated tree (Fig. 5), and was unsupported and unplaced in the ITS tree (Fig. 6).

Substrate preference did not entirely explain species relationships within *Athelia*. This contradicts my prediction that the fungal pathogens from lichen material on the ground would be a different species than on lichens which were still epiphytic. However, one of the powers of phylogenetics lies in our ability to test our hypotheses – represented here as gene trees produced during this study. I tested the probability of alternative tree topologies using the Approximately Unbiased (AU) test (Shimodaira, 2002). I created alternative trees to reflect *a priori* patterns I had observed among my samples. Specifically that monophyly would be a reflection of substrate use at time of collection for each *Athelia* (Figs. 2-4). For instance, that all epiphytic lichen-associated specimens would form a single clade, with the same being true for all fallen lichen-associated specimens and all wood associated specimens. I then used the AU test to determine if the constrained alternative trees could be rejected ($p\text{-AU} < 0.05$) or not ($p\text{-AU} > 0.05$). Any tree

with a $p\text{-AU} < 0.05$ would lead me to believe that that tree shape probably cannot be produced with my data, and is a rejectable alternative. For the AU test the null hypothesis would be that all trees are equally probable explanations of my data.

None of the substrate constraints (Figs. 2-4) were found to be probable alternatives to the original topology on the basis that each $p\text{-AU} \leq 0.05$ (Table 7). This suggests that substrate use at time of collection is, by itself, not an adequate predictor of relationships between these species of *Athelia*.

As an additional measure to delimit species based on genetic variation, I calculated the nucleotide divergence between and within *Athelia* species' haplotypes. Average pairwise differences between the lichen-associated *Athelia* lineage and all other species groups was greater in EF1- α than ITS with values of 0.08715 and 0.07159 between Group II and Group I respectively (Tables 8 & 9), whereas ITS average pairwise distance values ranged from 0.01863–0.04392. The mean nucleotide differences within the lichen-associated *Athelia* lineage were comparatively similar for ITS and EF1- α at 0.02000 and 0.019128, respectively, and represent the lowest mean difference values within any group except for the ITS of Group II (0.0182). The slightly higher within-group differences for the lichen-associated *Athelia* lineage may be a reflection of the highly supported split of isolates SG441 and SG550 as being sister to the lichen-associated *Athelia* lineage (Fig. 5).

All of the lichen-associated *Athelia* producing mature basidiomata were collected in cold, wet months of mid-late winter, often in the presence of snow (Larsen et al., 1981; Plate 5; Table 1). At other times of the year, only asexual sclerotia or hyphae were detectable on rat-tailed *Bryoria* (Plate 6). Following the ANOVA (Table 10) and Tukey HSD post hoc test, specimens of the lichen-associated *Athelia* have significantly longer (mean: 51.68 μm , $\pm 0.24 \mu\text{m}$, max: 26.07

μm , min: 9.69 μm) and wider basidia (mean: 15.4 μm , ± 0.05 μm , max: 7.36 μm , min: 4.03 μm), longer sterigmata (mean: 4.37 μm , ± 0.13 μm , max: 12.39 μm , min: 1.06 μm), and wider basidiospores (mean: 3.26 μm , ± 0.05 μm , max: 6.09 μm , min: 2.2 μm) than the other specimens measured (Figs. 8 & 9). Considerable overlap of the morphological measurements between species groups can be seen in the NMDS with no distinct patterns emerging (Fig. 10). The lichen-associated *Athelia* lineage overlapped considerably in ordination space but not entirely with the other species groups. Distinguishing *A. acrospora* measurements from those in Group I, Group II, or the lichen-associated *Athelia* using the NMDS was not possible. It is important to note that certain morphological characteristics (e.g., basidiospore shape or presence/ absence of cystidia) could not be included in this form of analysis. Specimen VS 9717 was excluded from the NMDS because a complete number of measurements for hyphal diameter could not be obtained due to lack of usable material.

3.2 Patterns of host preference

Only lichens in the family Parmeliaceae collected for this study were found to be infected by *Athelia* (Table 11). Within Parmeliaceae, lichens in the genus *Bryoria* were most frequently encountered as hosts representing 62.5% of all collected infected lichens (Table 11). Among *Bryoria*, the majority of detected infections were found on individuals in section *Implexae*. A total of 94 new sequences of *Bryoria* sect. *Implexae* were produced for this study, including 20 ITS sequences, 36 IGS, and 38 GAPDH sequences (Table 12). The final concatenated alignment consisted of 2018 characters (ITS: 513; IGS: 391; GAPDH: 1024), with 469 variable and 118 parsimony-informative sites (Fig. 11). The optimal *a priori* partitioning scheme (based on AICc score and returned log likelihood value) was to segregate ITS, IGS, and individual codon

positions of GAPDH of *Bryoria* sect. *Implexae* with separate evolutionary models (Table 6).

Within *Bryoria* sect. *Implexae*, no species groups were preferred hosts over any other (Fig. 11; Table 13).

3.3 The mold as a cryptic symbiont

Of the 55 specimens screened, no healthy *Bryoria* tested positive for the cryptic presence of *Athelia*, whereas all six rattail positive controls produced *Athelia* sequences (Table 1; Fig. 5)

4 DISCUSSION

4.1 Rattails and *Athelia*

The results indicate that the formation of rat-tailed *Bryoria* is strongly associated with the infection and subsequent winter growth of a novel species of *Athelia*, provisionally presented here as *Athelia seborrheica* sp. nov. pending formal publication (see *Taxonomy* p. 21; Plate 6). This mold has been found to infect only lichens in the family Parmeliaceae. Members of *Bryoria* sect. *Implexae* were found to be most frequently infected (Table 11). *Athelia seborrheica* is found on lichens still epiphytic as well as those which have fallen to the ground. Some but not all infected ground material could be placed within *A. seborrheica* (Fig. 5). Several isolates (SG520, SG519, SG555, SG570, SG573) could be assigned to *Athelia acrospora* based on sequence data, though no developed basidiomata were observable to determine their morphological affinity (Fig. 5). The placement of one isolate in particular, SG518, was poorly resolved across the concatenated and ITS gene trees (Figs. 5 & 6). However, in the EF1- α tree SG518 was found as sister to Group I/ *A. epiphylla* with significant bootstrap support (Fig. 7). The behavior of SG518 sequences across the three trees may be a reflection of incomplete lineage sorting or

incongruence between the gene trees generated (Dávalos et al., 2012), or could reflect poor quality of the ITS sequence for this isolate. If the former issue is true, then sampling additional loci, adding more taxa, or evaluating different character states for *Athelia* could resolve the unsupported relationships in these trees (Dávalos et al., 2012).

It is important to note that epiphytic *Bryoria* thalli can be classified in two ways: those which are anchored to the bark of the tree, and those which have fallen from above and have become draped over lower branches (Goward, 1998). Draped *Bryoria* falling from the upper canopy onto lower branches of the tree occupy a suboptimum habitat (Goward, 1998; Goward, 2003). Therefore, draped *Bryoria* might be more preferentially infected than those anchored, but because I did not classify my collections as draped or attached at the time they were collected I cannot address this with certainty. Whether lichens higher in the canopy are infected by *Athelia* or other fungi is unknown. Additionally, lichen decomposition could be a successional process. While *A. seborrheica* may initially degrade epiphytic lichen thalli, other microbes may be responsible for the later stages of its eventual breakdown once it reaches the ground (Coxson & Curteanu, 2002). *A. seborrheica* collected from fallen lichen thalli could have been present earlier in this successional process.

From sequence data, *A. seborrheica* seemed most closely related to *A. acrospora*, a wood decaying fungus not previously known to infect lichens, and *A. epiphylla*, the type species of the genus. Once reproductive individuals were found, the basidiospores and basidia of *A. seborrheica* were easily differentiated from *A. acrospora* in that the basidiospores of *A. acrospora* are much longer than wide (Jülich, 1972; Jülich & Stalpers, 1980) and its basidia are often smaller than what was observed in specimens of *A. seborrheica* (Table 14; Plate 6). The basidia of *A. epiphylla* are slightly shorter and wider than *A. seborrheica*, and *A. epiphylla* has

basidiospores which are larger and narrower than *A. seborrheica*. *Athelia arachnoidea*, another commonly reported lichen pathogen, is also easily distinguished morphologically from *A. seborrheica*. *Athelia arachnoidea* is often two-sterigmate, and has much larger basidiospores and basidia than *A. seborrheica* (Table 14; Jülich, 1972; Jülich & Stalpers, 1980).

The monophyly of *A. acrospora* or *A. epiphylla* was not supported in any tree produced in this study. Indeed, *A. epiphylla* represents a species complex in need of revision, the broad range of morphological forms of which could be mistaken for other species including but not limited to *A. acrospora* and *A. arachnoidea* (Jülich, 1972; Eriksson & Ryvarde, 1973; Jülich & Stalpers, 1980; Ginns & Worrall, 1999; Hawksworth, 2003). The polyphyletic nature of the other *Athelia* species may be a reflection of errors introduced by misidentification of herbarium material and GenBank deposits (Hofstetter et al., 2019). I was unable to examine type material of *A. epiphylla* (National Herbarium of the Netherlands in Leiden) or *A. acrospora* (Swedish Museum of Natural History in Stockholm), or GenBank vouchers UC2022957, UC 2022961, UC 2022960, UC 2022956, and UC 2022976 (University of California, Berkeley) because these specimens were unavailable for loan. *Athelia epiphylla* merits a proper phylogenetic re-examination (V. Spirin, University of Helsinki, pers. comm.) but that is beyond the scope of this study.

Knowing the species relationships and evolutionary history of *Athelia* is fundamental to follow-up investigations regarding this cosmopolitan genus of pathogens. Several species of *Athelia* are known as facultative pathogens of lichens (Diederich et al., 2018), but *Athelia* also contains economically important agricultural pests (Adams & Kropp, 1996). However, little phylogenetic information on this genus is available save studies on crop pests (Harlton et al., 1995; Adams & Kropp, 1996; Okabe & Matsumoto, 2003; Xu et al., 2010), a study of all

homobasidiomycetes associated with lichens in which *A. arachnoidea* was the only *Athelia* species included (Lawrey et al., 2007), and a report of an *Athelia* whose sclerotia – or asexual hyphal masses – mimic termite eggs (Matsuura et al., 2000). The phylogenetic trees produced in this study represent the largest sample of *Athelia* and will help bridge significant knowledge gaps for this genus.

It has been reported that *A. arachnoidea* depletes lichen thalli of nutrients via haustorial contact with the algal symbionts (Yurchenko & Golubkov, 2003). I was unable to determine how *Athelia seborrheica* was obtaining nutrients as no haustoria were visible from any of the microscopy that was performed during the course of this study. Lawrey and Diederich (2003) hypothesize that generalist parasites, such as *Athelia*, could possess a wide range of enzymes for the digestion of commonly found host material. Two groups of enzymes have been characterized in *Athelia (Sclerotia) rolfsii* and appear to play a key role in its infection of plant cellular material: cellobiose dehydrogenases (Baminger et al., 2001) and mannanases (Großwindhager et al., 1999). Cellobiose dehydrogenases are found in many wood-degrading species of fungi and are principally involved in the degradation of cellulose and/ or lignin (Baminger et al., 2001). The expression of mannan-degrading enzymes in *Athelia rolfsii* can be induced when glucose is the form of carbon available to fungal cultures of the pathogen (Großwindhager et al., 1999). However, other classes of mannanases can be expressed only when *A. rolfsii* is grown in cellulose media, indicating that the mold possesses a complex suite of enzymes to continuously degrade host material as different carbon sources are gradually used up (Großwindhager et al., 1999). It is unknown how *A. seborrheica* gains nutrients from its host. It could be parasitizing the photosynthesizing partner and/or fungal partners, or it might be tapping into the mannans, or other polysaccharides, which comprise the extracellular matrix of the lichen cortex (Spribille et

al., 2020). Alternatively it could be performing a combination of the three: moving from one nutritional aspect of its host to the next as it slowly exhausts each portion of the lichen (Plate 4).

4.2 *Bryoria* section *Implexae*

The majority of lichens found to be infected by *Athelia seborrheica* belonged to *Bryoria* sect. *Implexae* (Table 11). Differentiating individual species in this section relies on a balance of chemical, ecological, morphological, and molecular techniques (Velmala et al., 2014; Boluda et al. 2015, 2019). However, as is the case with most lichenological studies, molecular techniques are often employed for only the main mycobiont, or fungal partner, as a proxy for the lichen as a whole (Spribille, 2018). A previous study on *Bryoria* sect. *Implexae* found relationships within this group could be explained by broad geographical patterns as well as chemistry and morphology (Velmala et al., 2014), specifically that the lecanoromycete can be split into clades which are either European, North American, or more globally distributed (Velmala et al., 2014). Species concepts and data (i.e., sequences, chemistry, and morphology) from that study (Velmala et al., 2014) were the basis for the phylogenetic approach I used to determine which species of *Bryoria* sect. *Implexae* I had collected (Tables 4 & 13). However, the concatenated tree that I generated failed to support the same geographical distributions as being explanatory for species identity within sect. *Implexae* (Fig. 11). Additionally, no patterns of chemistry or morphology were reflected in the concatenated tree (Table 13; Fig. 11). The loci that I used (ITS, IGS, and GAPDH) appear to be under-informative. It could be argued that providing additional loci for the main mycobiont may be a useful way to disentangle this group more fully. However, when a recent study expanded the molecular dataset with two additional loci (FRBi15 and FRBi16) and

18 microsatellite markers, the authors still found a major mismatch between genetic relationships and the phenotypes of these *Bryoria* (Boluda et al., 2019).

Many of the species formerly accepted in *Bryoria* sect. *Implexae* have been synonymized with *B. fuscescens* (Boluda et al., 2019), though the chemical and morphological variation in *B. fuscescens* remains unexplained. It is apparent that the diverse chemistry, ecology, and morphology within *Bryoria* sect. *Implexae* have not been elucidated by previous phylogenies of the mycobiont (Boluda et al., 2015, 2019), a phenomenon Spribille (2018) referred to as the "phantom phenotype". To examine the lichen only in terms of its mycobiont is to miss the entire symbiosis it embodies (Goward, 2008). Surveying additional symbionts associated with *Bryoria* sect. *Implexae* – yeasts, bacteria, algae – could help to disentangle the evolutionary history of this group of lichens (Spribille, 2018).

4.3 Cryptic symbiosis

Athelia does not appear to be a cryptic, asymptomatic partner in hair lichen symbioses. I tested whether this fungal pathogen could be a dormant, potentially mutualistic or commensal partner that only begins to infect *Bryoria* as a result of some intrinsic symbiotic imbalance. This does not appear to be the case for *Athelia* since no healthy looking hair lichen tested positive for the presence of this fungus. I was driven to this line of investigation by recent studies that have found basidiomycete yeasts embedded within the cortices of ascomycete lichens, raising important questions regarding the nature of lichen symbiosis (Spribille et al., 2016, Tuovinen et al., 2019). I only tested for the presence of *Athelia*; whether other fungal pathogens could be intrinsic to these symbioses remains to be investigated.

5 CONCLUSION

Here I provide the first report of the pathogenic infection of *Bryoria* by a new species of mold, *Athelia seborrheica*. Whether or not this widespread infection of *Bryoria* in western North America is a recent event or simply an overlooked phenomenon is difficult to determine with certainty since using historical collections to assess the health of *Bryoria* over time was unfeasible for this study. Understanding the health of *Bryoria* and other hair lichens is essential to understanding the health of the forests they inhabit and the animals with which they interact, notably the herds of woodland caribou which depend upon them as a crucial winter food source (Edwards et al., 1960; Rominger et al., 1996; Thomas et al., 1996; Johnson et al., 2000). This research serves as the historic benchmark for documenting a pathogenic outbreak affecting an ecologically significant lichen genus.

6 TAXONOMY

Athelia seborrheica Goyette & T. Sprib. **sp. nov.**

Type: USA, Montana, Edna Creek Rd. area (48°40.391'N, 115°01.109'W), on *Bryoria* section *Implexae* epiphytic on *Abies lasiocarpa*, 7 April 2019, S. Goyette 633 (DNA isolate SG524; holotype: University of Alberta Herbarium [ALTA]; isotypes: Canadian Museum of Nature [CANL], University of Helsinki [H])

Diagnosis

Differing from *Athelia arachnoidea* in its shorter basidia usually with four sterigmata, from *A. acrospora* in its stouter basidiospores, and from *A. epiphylla* in its slightly longer though narrower basidia, wider basidiospores, and preferential infection of hair lichens in Parmeliaceae.

Description

Basidiomata effuse. Hymenial surface cottony, eggshell to creamy white. Context white, thin (<100 µm), texture indistinct. Margin white, densely cottony to arachnoid, hyphal strands present. Hymenial surface whitish, indistinct. Hyphae monomitic with clamps at septa. Hyphae hyaline, cylindrical, 2–3 µm in diameter, rarely encrusted with crystals. Cystidia absent. Basidia hyaline, cylindrical to clavate when mature, 14–18.5–(20) x 5.5–6–(7) µm, smooth surfaced, with four – seldom two – equally elongate sterigmata 3.5–5.5 x 1–1.5 µm. Basidiospores thin-walled, hyaline, ovate with rounded base and prominent apiculus, 4.5–5.5 x 3–3.5–(4.5) µm, occasionally sticking together.

Habitat

Preferred substrates are hair lichens in the Parmeliaceae, specifically *Bryoria* sect. *Implexae*. Seldom found on bark of *Abies lasiocarpa* in lichen-rich forests. Abundant in western North America with one specimen lacking a basidioma (isolate SG624) from eastern Sweden.

Etymology

From seborrhea, a discharge of oily matter which can manifest as a severe form of dandruff characterized by inflammation and flaking of skin from the scalp, nose, and eyebrows.

Commentary

GenBank accession KP814332 represents an ITS sequence from specimen UC 2022957 (Rosenthal et al., 2017) derived from "litter or well decayed wood in pinaceous forest" and was collected in Oregon, USA. This specimen was requested on loan but was unavailable for study. The sequence differs in 1 position and is likely referable to *A. seborrheica*.

Additional Specimens Examined (*Athelia seborrheica*):

CANADA. ALBERTA: Athabasca County, 4 Jun 2018, S Goyette 522 (DNA isolate SG426); ~1-1.5 km from HWY to Fort McMurray backroad, 20 Apr 2018, S Goyette 299 (DNA isolate SG410); Lily Lake Trail, 25 May 2019, T Spribille (DNA isolate SG567); Marten Lakes Wilderness Campus, 22 Sep 2018, S Goyette 581 (DNA isolate SG441); Marten Lakes

Wilderness Campus, 23 Sep 2018, S Goyette 583 (DNA isolate SG436); Marten Lakes Wilderness Campus, 21 Sep 2019, S Goyette 648 (DNA isolate SG641); before Marlboro, 23 Feb 2018, S Goyette 625 (DNA isolate SG493); Mukiki Lake, 18 May 2019, S Goyette 638 (DNA isolate SG542); Mukiki Lake, 18 May 2019, S Goyette 643 (DNA isolate SG564); outside of Mukiki Lake, 18 May 2019, S Goyette 641 (DNA isolate SG562); north of Rock Island Lake, 26 Apr 2019, T Spribille (DNA isolate SG560); off HWY 43 before Whitecourt, 10 Jul 2018, S Goyette 536 (DNA isolate SG450); Yellowhead County, 18 May 2019, S Goyette 639 (DNA isolate SG548); Yellowhead County, 18 May 2019, S Goyette 640 (DNA isolate SG550).

BRITISH COLUMBIA: outside Chinook Cove, T Spribille (DNA isolate SG455); outside Chinook Cove, T Spribille (DNA isolate SG459); outside Chinook Cove, T Spribille (DNA isolate SG461); Crystal Ridge area, Valemount, 17 Mar 2019, S Goyette 627 (DNA isolate SG505); Coquihalla Pass, 11 May 2019, T Spribille (DNA isolate SG556); Coquihalla Pass, 11 May 2019, T Spribille (DNA isolate SG558); Coquihalla Pass, 11 May 2019, T Spribille (DNA isolate SG572); past Falkland, T Spribille (DNA isolate SG456); past Falkland, T Spribille (DNA isolate SG458); past Falkland, T Spribille (DNA isolate SG460); Little Lost Lake trail loop, 11 May 2019, S Goyette 646 (DNA isolate SG635); Upper Clearwater Valley, 28 Aug 2019, T. Goward 19-154 (DNA isolate SG653); Upper Clearwater Valley, 28 Aug 2019, T. Goward 19-155 (DNA isolate SG656).

SWEDEN: UPPLAND, Vänge parish, T Spribille (DNA isolate SG624).

USA. IDAHO: outside of Lolo Pass, S Goyette 626 (DNA isolate SG498).

MONTANA: Edna Creek Rd. area, 7 Apr 2019, S Goyette 631 (DNA isolate SG512); Edna Creek Rd. area, 7 Apr 2019, S Goyette 636 (DNA isolate SG527); Edna Creek Rd. area, 7 Apr 2019, S Goyette 637 (DNA isolate SG528); outside Edna Creek Rd. area, 7 Apr 2019, S Goyette 632 (DNA isolate SG521); outside Edna Creek Rd. area, 6 Apr 2019, S Goyette 634 (DNA isolate SG525); outside Stryker, 6 Apr 2019, S Goyette 629 (DNA isolate SG507); outside Stryker, 6 Apr 2019, S Goyette 635 (DNA isolate SG526); outside Stryker/ Stillwater, 6 Apr 2019, S Goyette 645 (DNA isolate SG574); outside of Stryker, 6 Apr 2019, S Goyette 628 (DNA isolate SG506); outside of Stryker, 6 Apr 2019, S Goyette 630 (DNA isolate SG510).

WASHINGTON: Clallam Co., Hurricane Ridge, 19 Sep 2014, VS 8747 (DNA isolate SG588).

Note: All specimens are deposited in ALTA except T. Goward 19-154 (DNA isolate SG653) and T. Goward 19-155 (DNA isolate SG656), which are in the Beaty Biodiversity Museum [UBC].

Comparison Material Examined (*Athelia acrospora*):

CANADA. ALBERTA: outside Nojack, 9 May 18, S Goyette 393 (DNA isolate 414). BRITISH COLUMBIA: Coquihalla Pass, C, 11 May 2019, T Spribille (DNA isolate SG555); Coquihalla Pass, 11 May 19, T Spribille (DNA isolate SG573); outside Lower Goat River Trail, 12 May 19, S Goyette 644 (DNA isolate SG570); Trophy Mountain, 9 Jun 18, S Goyette 525 (DNA isolate SG357). SASKATCHEWAN: near La Ronge, 28 Apr 18, T Spribille (DNA isolate SG519); near La Ronge, 28 Apr 18, T Spribille (DNA isolate SG520). USA. WASHINGTON: Pend Oreille Co., Gypsy Meadows, 17 Oct 2014, VS 8701a (DNA isolate SG586).

Comparison Material Examined (*Athelia arachnoidea*):

AUSTRIA. STYRIA: Kainbach bei Voitsberg, T Spribille (DNA isolate SG621).

Comparison Material Examined (*Athelia bombacina*):

CANADA. ALBERTA: outside of Mukiki Lake, 18 May 19, S Goyette 642 (DNA isolate SG563).

Comparison Material Examined (*Athelia cystidiolophora*):

RUSSIA. NIZHNY NOVGOROD REGION: Lukoyanov Dist., Panzelka 26 July 2018, VS 12063 (DNA isolate SG601); Bogorodsk Dist., Krastelikha 5 Sept 2011, VS 4442 (DNA isolate 603). LENINGRAD REGION: Podporozhie Dist., Vazhinka, 16 Sept 2017, VS 11390 (DNA isolate SG600).

Comparison Material Examined (*Athelia decipiens*):

RUSSIA. KHABAROVSK REGION: Verkhnebureinskii Dist., Kyvyty 17 Aug 2014, VS 7395 (DNA isolate SG597). NIZHNY NOVGOROD REGION: Bogorodsk Dist., Krastelikha 2 Oct 2015, VS 9867 (DNA isolate SG604); Lukoyanov Dist., Sanki 20 Aug 2015, VS 9737 (DNA isolate SG610); Lukoyanov Dist., Sanki Reg., 4 Aug 2017, VS 11357 (DNA isolate SG596).

Comparison Material Examined (*Athelia epiphylla*):

CANADA. ALBERTA: East of Devon, Small tributary of North Sask River, 16 June 1999, UA10144 (DNA isolate SG615); Yellowhead County, Whitehorse Wildland Provincial Park, 26 July 2015, VS 8961 (DNA isolate SG582); Yellowhead County, Whitehorse Wildland Provincial Park, 26 July 2015, VS 8958 (DNA isolate SG593). RUSSIA. LENINGRAD REGION: Boksitogorsk Dist., Chagoda, 9 May 2018, VS 11884 (DNA isolate SG595). NIZHNY NOVGOROD REGION: Boksitogorsk Dist., Chagoda 9 May 2018, VS 11884 (DNA isolate SG595); Lukoyanov Dist., Sanki, 20 Aug 2015, VS 9719 (DNA isolate SG594).

Comparison Material Examined (*Athelia* sp.):

CANADA. ALBERTA: in string fen near Lac La Biche, S Goyette 647 (DNA isolate SG639).

SASKATCHEWAN: near La Ronge, 28 Apr 18, T Spribille (DNA isolate SG518).

Note: ITS and EF1- α sequences from specimen S Goyette 647 (DNA isolate SG639) were sister to *A. arachnoidea* sequences in all gene trees. The length of the branch between this specimen and the *A. arachnoidea* was long suggesting that it represents a separate species. No mature basidiomata were present to determine the identity of this specimen.

7 TABLES, FIGURES, and PLATES

Table 1 Voucher table for *Athelia* collected and sequenced for this study. Type specimen for *Athelia seborrheica* (S Goyette 633, extraction number SG524) is in bold. Final GenBank accession numbers for the ITS and EF1- α will be obtained upon formal submission of the publication. Successfully sequenced loci are indicated with an "x".

<u>Genus species</u>	<u>Extract ID</u>	<u>Locality</u>	<u>Elevation (m)</u>	<u>Collection number</u>	<u>Substrate</u>	<u>Lichen Host</u>	<u>Latitude</u>	<u>Longitude</u>	<u>Basidioma measured?</u>	<u>ITS</u>	<u>EF1-α</u>	<u>Notes</u>
<i>Athelia seborrheica</i>	SG410	~1-1.5 km from HWY to Fort McMurray (backroad), Alberta, 20 Apr 2018	592	S Goyette 299	lichen/epiphyte	<i>Bryoria</i> sect. <i>Implexae</i>	55°23.596' N	112°28.396'W	No	x		a priori collection and extraction
<i>Athelia seborrheica</i>	SG426	Athabasca County, Alberta, 4 Jun 2018	539	S Goyette 522	lichen/epiphyte	<i>Bryoria</i> sect. <i>Implexae</i>	54°57.056' N	112°57.280'W	No	x		a priori collection and extraction
<i>Athelia seborrheica</i>	SG436	Marten Lakes Wilderness Campus, Alberta, 23 Sep 2018	800	S Goyette 583	lichen/ground	<i>Bryoria</i> and <i>Usnea</i>	55°36'35.0"N	114°33'35.0"W	No	x	x	

<i>Athelia seborrheica</i>	SG450	off HWY 43 before Whitecourt, Alberta, 10 Jul 2018	700	S Goyette 536	lichen/epiphyte	<i>Bryoria fuscescens</i>	54°06'16.5"N	115°37'39.0"W	No	x		a priori collection and extraction
<i>Athelia seborrheica</i>	SG455	outside Chinook Cove, British Columbia	760	T Spribille	lichen/epiphyte	<i>Bryoria</i> sect. <i>Implexae</i>	51°15'31.2"N	120°12'44.7"W	No	x	x	
<i>Athelia seborrheica</i>	SG456	past Falkland, British Columbia	810	T Spribille	lichen/epiphyte	<i>Bryoria</i> sect. <i>Implexae</i> and <i>Usnea</i>	50°26'08.4"N	119°30'17.7"W	No	x	x	
<i>Athelia seborrheica</i>	SG458	past Falkland, British Columbia	810	T Spribille	lichen/epiphyte	<i>Bryoria</i> sect. <i>Implexae</i> and <i>Usnea</i>	50°26'08.4"N	119°30'17.7"W	No	x	x	
<i>Athelia seborrheica</i>	SG459	outside Chinook Cove, British Columbia	760	T Spribille	lichen/epiphyte	<i>Bryoria</i> sect. <i>Implexae</i>	51°15'31.2"N	120°12'44.7"W	No	x	x	

<i>Athelia seborrheica</i>	SG460	past Falkland, British Columbia	760	T Spribille	lichen/epiphyte	<i>Bryoria sect. Implexae</i>	51°15'31.2"N	120°12'44.7"W	No	x	x	
<i>Athelia seborrheica</i>	SG461	outside Chinook Cove, British Columbia	810	T Spribille	lichen/epiphyte	<i>Bryoria tortuosa</i> and <i>Bryoria sect. Implexae</i>	50°26'08.4"N	119°30'17.7"W	No	x	x	
<i>Athelia seborrheica</i>	SG493	before Marlboro, Alberta , 23 Feb 2018	997	S Goyette 625	lichen/epiphyte	<i>Bryoria fremontii</i>	53°34.065' N	116°42.204'W	Yes	x	x	
<i>Athelia seborrheica</i>	SG498	outside of Lolo Pass, Idaho	1280	S Goyette 626	lichen/epiphyte	<i>Bryoria fremontii</i> and <i>Bryoria fuscescens</i>	46°47'05.7"N	114°23'02.1"W	No	x	x	
<i>Athelia seborrheica</i>	SG505	Crystal Ridge area, Valemount, British Columbia, 17 Mar 2019	960	S Goyette 627	lichen/epiphyte	<i>Bryoria sect. Implexae</i>	52°47'25.7"N	119°17'30.3"W	No	x		

<i>Athelia seborrheica</i>	SG506	outside of Stryker, Montana, 6 Apr 2019	1006	S Goyette 628	lichen/epiphyte	<i>Bryoria fremontii</i> and <i>Bryoria fuscescens</i>	48°40.302' N	114°45.297'W	No	x	x	
<i>Athelia seborrheica</i>	SG507	outside Stryker, Montana, 6 Apr 2019	1211	S Goyette 629	lichen/epiphyte	<i>Bryoria sect. Implexae</i>	48°41.510' N	114°44.173'W	No	x	x	
<i>Athelia seborrheica</i>	SG510	outside of Stryker, Montana, 6 Apr 2019	1211	S Goyette 630	lichen/epiphyte	<i>Bryoria sect. Implexae</i> and <i>Nodobryoria oregana</i>	48°41.510' N	114°44.173'W	No	x	x	
<i>Athelia seborrheica</i>	SG512	Edna Creek Rd. area, Montana, 7 Apr 2019	1352	S Goyette 631	lichen/epiphyte	<i>Bryoria fuscescens</i>	48°40.391' N	115°01.109'W	Yes	x		
<i>Athelia seborrheica</i>	SG521	outside Edna Creek Rd. area, Montana, 7 Apr 2019	1352	S Goyette 632	lichen/epiphyte	<i>Bryoria sect. Implexae</i> and <i>Hypogymnia</i>	48°40.391' N	115°01.109'W	Yes	x	x	

<i>Athelia seborrheica</i>	SG524	on <i>Abies lasiocarpa</i> , Edna Creek Rd. area, Montana, 7 Apr 2019	1352	S Goyette 633	lichen/epiphyte	<i>Bryoria</i> sect. <i>Implexae</i>	48°40.391' N	115°01.109'W	Yes	x	x	
<i>Athelia seborrheica</i>	SG525	outside Edna Creek Rd. area, Montana, 6 Apr 2019	1211	S Goyette 634	lichen/epiphyte	<i>Bryoria</i> sect. <i>Implexae</i> and <i>Nodobryoria oregana</i>	48°41.510' N	114°44.173'W	Yes	x	x	
<i>Athelia seborrheica</i>	SG526	outside Stryker, Montana, 6 Apr 2019	1211	S Goyette 635	lichen/epiphyte	<i>Bryoria</i> sect. <i>Implexae</i>	48°41.510' N	114°44.173'W	Yes	x		
<i>Athelia seborrheica</i>	SG527	Edna Creek Rd. area, Montana, 7 Apr 2019	1352	S Goyette 636	lichen/epiphyte	<i>Bryoria</i> sect. <i>Implexae</i>	48°40.391' N	115°01.109'W	Yes	x	x	
<i>Athelia seborrheica</i>	SG528	Edna Creek Rd. area, Montana, 7 Apr 2019	1352	S Goyette 637	lichen/epiphyte	<i>Bryoria</i> sect. <i>Implexae</i>	48°40.391' N	115°01.109'W	Yes	x	x	

<i>Athelia seborrheica</i>	SG542	Mukiki Lake, Alberta, 18 May 2019	1580	S Goyette 638	lichen/ground	<i>Bryoria</i> , <i>Usnea</i> , and <i>Hypogymnia</i>	52°50.678' N	116°51.71 5'W	No	x	x	
<i>Athelia seborrheica</i>	SG548	Yellowhead County, Alberta, 18 May 2019	1935	S Goyette 639	lichen/epiphyte	<i>Bryoria simplicior</i> , <i>Bryoria fuscescens</i> , and <i>Usnea</i>	52°53.110' N	116°58.89 1'W	No	x	x	
<i>Athelia seborrheica</i>	SG556	Coquihalla Pass, British Columbia, 11 May 2019	1220	T Spribille	lichen/ground	<i>Alectoria sarmentosa</i>	49°35'38.2 "N	121°07'16 .8"W	No	x		
<i>Athelia seborrheica</i>	SG558	Coquihalla Pass, British Columbia, 11 May 2019	1220	T Spribille	lichen/ground	<i>Alectoria sarmentosa</i>	49°35'38.2 "N	121°07'16 .8"W	No	x	x	
<i>Athelia seborrheica</i>	SG560	north of Rock Island Lake, Alberta, 26 Apr 2019	770	T Spribille	lichen/ground	<i>Bryoria</i> , <i>Evernia mesomorpha</i> , and <i>Usnea</i>	55°34.958' N	113°27.01 0'W	No	x	x	

<i>Athelia seborrheica</i>	SG562	outside of Mukiki Lake, Alberta, 18 May 2019	1935	S Goyette 641	lichen/ground	<i>Bryoria</i> sect. <i>Implexae</i>	52°53.110' N	116°58.891'W	No	x		
<i>Athelia seborrheica</i>	SG564	Mukiki Lake, Alberta, 18 May 2019	1580	S Goyette 643	lichen/ground	<i>Bryoria</i> sect. <i>Implexae</i> and <i>Usnea</i>	52°50.678' N	116°51.715'W	No	x		
<i>Athelia seborrheica</i>	SG567	Lily Lake Trail, Alberta, 25 May 2019	970	T Spribille	lichen/epiphyte	<i>Bryoria pikei/capillaris</i> and <i>Usnea</i>	55°28'01.3"N	114°42'49.1"W	No	x		
<i>Athelia seborrheica</i>	SG572	Coquihalla Pass, British Columbia, 11 May 2019	1220	T Spribille	lichen/epiphyte	<i>Alectoria</i> , <i>Platismatia</i> , and <i>Hypogymnia</i>	49°35'38.2"N	121°07'16.8"W	No	x	x	
<i>Athelia seborrheica</i>	SG574	outside Stryker/Stillwater, Montana, 6 Apr 2019	1211	S Goyette 645	lichen/epiphyte	NA	48°41.510' N	114°44.173'W	No	x	x	

<i>Athelia seborrheica</i>	SG624	Uppland, Vänge parish, 5.5 km NW of Vänge village, 25 m W of the border to the nature reserve Fiby Urskog, Sweden	130	T Spribille	lichen/epiphyte	<i>Bryoria</i> sect. <i>Implexae</i>	59°52'51.7"N	17°21'05.9"E	No	x		
<i>Athelia seborrheica</i>	SG635	Little Lost Lake trail loop, British Columbia, 11 May 2019	800	S Goyette 646	lichen/epiphyte	<i>Bryoria</i> sect. <i>Implexae</i>	55°36'36.5"N	114°34'11.6"W	No	x		
<i>Athelia seborrheica</i>	SG641	Marten Lakes Wilderness Campus, Alberta, 21 Sep 2019	800	S Goyette 648	lichen/epiphyte	<i>Usnea</i>	55°36'35.0"N	114°33'35.0"W	Yes	x		
<i>Athelia seborrheica</i>	SG653	Philip Creek drainage: 1 km west of Philip Lake, Upper Clearwater Valley, British Columbia, 28 Aug 2019	1600	T. Goward 19-154	lichen/epiphyte	<i>Bryoria glabra</i>	51°52'15.4"N	119°55'02.3"W	No	x		

<i>Athelia seborrheica</i>	SG656	26 km north of Clearwater Village: 1 km w of "Edgewood Blue", Upper Clearwater Valley, British Columbia, 28 Aug 2019	715	T. Goward 19-155	lichen/epiphyte	<i>Bryoria</i> sect. <i>Implexae</i>	51°52'09.7"N	120°01'18.0"W	No	x		
<i>Athelia seborrheica</i>	SG588	Hurricane Ridge, Clallam Co., Washington (fallen log), 19 Sep 2014	1645	VS 8747	Wood; fallen log	NA	47°56'01.2"N	123°24'23.2"W	Yes	x		
<i>Athelia aff. seborrheica</i>	SG441	Marten Lakes Wilderness Campus, Alberta, 22 Sep 2018	800	S Goyette 581	lichen/epiphyte	<i>Bryoria</i> sect. <i>Implexae</i>	55°36'36.5"N	114°34'11.6"W	No	x		a priori collection and extraction
<i>Athelia aff. seborrheica</i>	SG550	Yellowhead County, Alberta, 18 May 2019	1935	S Goyette 640	lichen/ground	<i>Bryoria</i> sect. <i>Implexae</i> and <i>Usnea</i>	52°53.110' N	116°58.891'W	No	x	x	

<i>Athelia acrospora</i> Jülich	8230	Scandinavia		K-H Larsson		NA			No	x		
<i>Athelia acrospora</i> Jülich	SG357	Trophy Mountain, British Columbia, 9 Jun 18	1802	S Goyette 525	lichen/ epiphyte	<i>Bryoria sect.</i> <i>Implexae</i>	51°45.611' N	119°56.28 7'W	No	x		a priori collection and extraction
<i>Athelia acrospora</i> Jülich	SG414	outside Nojack, Alberta, 9 May 18	821	S Goyette 393	lichen/ epiphyte	<i>Bryoria</i> <i>(subcana)</i> <i>fuscesens</i>	53°35.070' N	115°37.34 1'W	No	x		a priori collection and extraction
<i>Athelia acrospora</i> Jülich	SG519	near La Ronge, Saskatchewan , 28 Apr 18	446	T Spribille	lichen/ ground	<i>Bryoria</i> , <i>Evernia</i> <i>mesomorpha</i> , and <i>Usnea</i>	55°06.987' N	105°15.14 1'W	No	x		
<i>Athelia acrospora</i> Jülich	SG520	near La Ronge, Saskatchewan , 28 Apr 18	446	T Spribille	lichen/ ground	<i>Bryoria</i> , <i>Evernia</i> <i>mesomorpha</i> , and <i>Usnea</i>	55°06.987' N	105°15.14 1'W	No	x		

<i>Athelia acrospora</i> Jülich	SG555	Coquihalla Pass, British Columbia, C, 11 May 2019	1220	T Spribille	lichen/ground	<i>Alectoria sarmentosa</i>	49°35'38.2"N	121°07'16.8"W	No	x		
<i>Athelia acrospora</i> Jülich	SG570	outside Lower Goat River Trail, British Columbia, 12 May 19	1420	S Goyette 644	lichen/ground	<i>Bryoria, Alectoria, and Usnea</i>	53°26'43.0"N	120°39'21.0"W	No	x		
<i>Athelia acrospora</i> Jülich	SG573	Coquihalla Pass, British Columbia, 11 May 19	1220	T Spribille	lichen/ground	<i>Platismatia</i>	49°35'38.2"N	121°07'16.8"W	No	x		
<i>Athelia acrospora</i> Jülich	SG586	Gypsy Meadows, Pend Oreille Co., Washington 17 Oct 2014	1310	VS 8701a	wood; fallen log	NA	48°54'15.0"N	117°04'45.3"W	Yes	x	x	
<i>Athelia arachnoidea</i> (Berk.) Jülich	SG621	Kainbach bei Voitsberg, Austria	1170	T Spribille	lichen/epiphyte	<i>Bryoria, Pseudevernia furfuracea, and Usnea</i>	47°10'04.3"N	14°58'13.9"E	No	x		

<i>Athelia cf. arachnoidea</i>	SG639	in string fen near Lac La Biche, Alberta	690	S Goyette 647	lichen/ground	<i>Bryoria fuscescens</i> , <i>Usnea</i> , and <i>Hypogymnia</i>	55°15'19.8 "N	111°18'47 .4"W	No	x		
<i>Group I – Athelia bombacina</i> Pers.	SG563	outside of Mukiki Lake, Alberta, 18 May 19	1935	S Goyette 642	wood	NA	52°53.110' N	116°58.89 1'W	No	x		
<i>Group I – Athelia epiphylla</i> Pers.	SG582	Whitehorse Wildland Provincial Park, Yellowhead Co., Alberta, 26. July 2015	1610	VS 8961	wood	NA	52°59'01.2 "N	117°20'48 .3"W	Yes	x	x	
<i>Group I – Athelia epiphylla</i> Pers.	SG593	Whitehorse Wildland Provincial Park, Yellowhead Co., Alberta, 26. July 2015	1610	VS 8958	wood	NA	52°59'01.2 "N	117°20'48 .3"W	Yes	x	x	
<i>Group I – Athelia epiphylla</i> Pers.	SG615	Small tributary of North Sask River, East of Devon, Alberta, 16 June 1999	680	UA10144	wood	NA	53°21'19.9 "N	113°42'36 .0"W	Yes	x		

<i>Group I – Athelia sp.</i>	SG518	near La Ronge, Saskatchewan, 28 Apr 18	446	T Spribille	lichen/ground	<i>Bryoria, Evernia mesomorpha, and Usnea</i>	55°06.987' N	105°15.141'W	No	x	x	
<i>Group II – Athelia cystidiolophora</i> Parm.	SG600	Vazhinka, Podporozhie Dist., Leningrad Reg., Russia, 16 Sept 2017	160	VS 11390	wood	NA	61°14'06.8 "N	33°52'40.9"E	Yes	x		
<i>Group II – Athelia cystidiolophora</i> Parm.	SG601	Panzelka, Lukoyanov Dist., Nizhny Novgorod Reg., Russia 26 July 2018	70	VS 12063	wood	NA	54°51'38.1 "N	44°20'40.6"E	No	x		
<i>Group II – Athelia cystidiolophora</i> Parm.	SG603	Krastelikha, Bogorodsk Dist., Nizhny Novgorod Reg., Russia, 5 Sept 2011	130	VS 4442	wood	NA	56°07'29.3 "N	43°27'14.3"E	Yes	x		
<i>Group II – Athelia decipiens</i> s.l. (v. Höhn. et Litsch.) J. Erikss.	SG604	Krastelikha, Bogorodsk Dist., Nizhny Novgorod Reg., Russia, 2 Oct 2015	130	VS 9867	wood	NA	56°07'29.3 "N	43°27'14.3"E	Yes	x		

<i>Group II – Athelia decipiens</i> s.l. (v. Höhn. et Litsch.) J. Erikss.	SG610	Sanki, Lukoyanov Dist., Nizhny Novgorod Reg., Russia, 20 Aug 2015	70	VS 9737	wood	NA	54°50'23.3 "N	44°13'44.7"E	Yes	x		
<i>Group II – Athelia decipiens</i> (v. Höhn. et Litsch.) J. Erikss.	SG596	Sanki, Lukoyanov Dist., Nizhny Novgorod Reg., Russia, 4 Aug 2017	70	VS 11357	wood	NA	54°50'23.3 "N	44°13'44.7"E	Yes	x	x	
<i>Group II – Athelia decipiens</i> (v. Höhn. et Litsch.) J. Erikss.	SG597	Kyvyty, Verkhneburei nskii Dist., Khabarovsk Reg., Russia, 17 Aug 2014	600	VS 7395	wood	NA	50°24'04.6 "N	133°13'39.0"E	Yes	x		
<i>Group II – Athelia epiphylla</i> s.l. Pers.	SG595	Chagoda, Boksitogorsk Dist., Leningrad Reg., Russia, 9 May 2018	40	VS 11884	wood	NA	59°08'51.4 "N	35°18'42.0"E	Yes	x	x	
<i>Group II – Athelia epiphylla</i> Pers.	SG594	Sanki, Lukoyanov Dist., Nizhny Novgorod Reg., Russia, 20 Aug 2015	70	VS 9719	wood	NA	54°50'23.3 "N	44°13'44.7"E	Yes	x		

Table 2 Atheliaceae voucher information from GenBank. When provided, substrate of *Athelia* was acquired from accession data. ITS and EFI- α refer to the GenBank accession numbers per specimen per locus. *Leptosporomyces raunkiaeri* (M.P. Christ) Jülich and *Piloderma fallax* (Lib.) Stalpers were chosen as outgroup taxa.

Species ID	Voucher ID	Substrate	Locality	ITS	EFI- α
<i>Athelia acrospora</i>	UC2022961	wood/ soil	California, USA	KP814228	-
<i>Athelia acrospora</i>	UC2022957	wood/ soil	Oregon, USA	KP814332	-
<i>Athelia acrospora</i>	UC2022976	wood/ soil	Montana, USA	KP814372	-
<i>Athelia acrospora</i>	UC2022956	wood/ soil	Montana, USA	KP814375	-
<i>Athelia acrospora</i>	UC2022960	wood/ soil	Montana, USA	KP814376	-
<i>Athelia arachnoidea</i>	UC2022900	wood/ soil	Montana, USA	KP814459	-
<i>Athelia arachnoidea</i>	CBS:105.18	unknown	Germany	KY025592	-
<i>Athelia arachnoidea</i>	CBS:418.72	unknown	Netherlands	MH860510	GU187672
<i>Athelia bombacina</i>	UC2023122	wood/ soil	Wyoming, USA	KP814299	-
<i>Athelia bombacina</i>	UC2023176	wood/ soil	Idaho, USA	KP814356	-
<i>Athelia bombacina</i>	UC2023189	wood/ soil	Montana, USA	KP814384	-
<i>Athelia bombacina</i>	UC2023159	wood/ soil	Montana, USA	KP814388	-
<i>Athelia bombacina</i>	UC2023173	wood/ soil	Montana, USA	KP814391	-
<i>Athelia decipiens</i>	NFLI 2000-87/10/1	unknown	unknown	JQ358800	
<i>Athelia decipiens</i>	CBS:103869	unknown	Finland	KY025593	-
<i>Athelia decipiens</i>	MO311848	wood	Tennessee, USA	MH558297	-
<i>Athelia decipiens</i>	FCUG 1762	unknown	unknown	U85797	-
<i>Athelia epiphylla</i>	SFC21080314-01	unknown	South Korea	MK992816	-
<i>Athelia epiphylla</i>	CFMR:FP-100564	wood	Maryland, USA	GU187501	GU187676
<i>Athelia arachnoidea</i>	ATCC 10866	unknown	unknown	U85789	-
<i>Leptosporomyces raunkiaeri</i>	CFMR:HHB-7628	wood	Michigan, USA	GU187528	GU187719
<i>Piloderma fallax</i>	CFMR:S-12	unknown	Wisconsin, USA	GU187535	GU187738

Table 3 List of primers used and/ or developed in this study to target *Athelia* internal transcribed spacer region (ITS) and translation elongation factor 1- α (EF1- α) used and/ or developed in this study, as well as host intergenomic spacer (IGS), glyceraldehyde-3-phosphate dehydrogenase (GAPDH), and ITS.

Gene Region	Abbreviation	5' – 3'	Source
ITS (forward)	Ath_ITS_F1	TATAAGGC TYTGATTG TGC	This study
ITS (reverse)	Ath_ITS_R1	AATGGTTT RTAAAATT GTCC	This study
EF1- α (forward)	Ath_EF1a_F4	AYGCYCTS TTGGCGTT CACYC	This study
EF1- α (reverse)	Ath_EF1a_R4	GCGACAGT TTGYCTCA TGTCACGG	This study
ITS (forward)	ITS1-F	CTTGGTCA TTTAGAGG AAGTAA	Gardes & Bruns (1993)
ITS (reverse)	ITS4	TCCTCCGC TTATTGAT ATGC	White et al. (1990)
EF1- α (forward)	EF983	GCYCCYGG HCAYCGTG AYTTYAT	Rehner & Buckley (2005)
EF1- α (reverse)	EF2218R	ATGACACC RACRGCRA CRGTYTG	Rehner & Buckley (2005)
IGS (forward)	IGS12B	AGTCTGTG GATTAGTG GCCG	Printzen & Ekman (2002)
IGS (reverse)	SSU72R	TTGCTTAA ACTTAGAC ATG	Gargas & Taylor (1992)
GAPDH (forward)	Gpd1-LM	ATTGGCCG CATCGTCT TCCGCAA	Myllys et al. (2002)
GAPDH (reverse)	Gpd2-LM	CCCACTCG TTGTGTA CCA	Myllys et al. (2002)

Table 4 Voucher information for *Bryoria* sect. *Implexae* ITS, IGS, and GAPDH sequences from GenBank. ITS, IGS, and GAPDH refer to the GenBank accession numbers per specimen per locus.

Genus species	Voucher ID	Source	ITS	IGS	GAPDH
<i>Bryoria capillaris</i> (Ach.) Brodo & D. Hawksw.	L141	Velmala et al., 2014	FJ668493	FJ668455	FJ668399
<i>Bryoria capillaris</i> (Ach.) Brodo & D. Hawksw.	L211	Velmala et al., 2014	GQ996287	KJ396487	GQ996259
<i>Bryoria capillaris</i> (Ach.) Brodo & D. Hawksw.	L270	Velmala et al., 2014	GQ996288	KJ396488	GQ996260
<i>Bryoria capillaris</i> (Ach.) Brodo & D. Hawksw.	S192	Velmala et al., 2014	GQ996289	KJ396490	GQ996261
<i>Bryoria capillaris</i> (Ach.) Brodo & D. Hawksw.	S2	Velmala et al., 2014	KJ396433	KJ396489	KJ954306
<i>Bryoria friabilis</i> Brodo & D. Hawksw.	L407	Velmala et al., 2014	KJ396435	KJ396492	KJ954308
<i>Bryoria friabilis</i> Brodo & D. Hawksw.	S395a	Velmala et al., 2014	KJ576728	KJ396493	KJ599481
<i>Bryoria friabilis</i> Brodo & D. Hawksw.	L355	Velmala et al., 2014	KJ396434	KJ396491	KJ954307
<i>Bryoria fuscescens</i> (Gyeln.) Brodo & D. Hawksw.	S260b	Velmala et al., 2014	GQ996286	KJ396508	GQ996258
<i>Bryoria fuscescens</i> (Gyeln.) Brodo & D. Hawksw.	L149	Velmala et al., 2014	GQ996290	KJ396496	GQ996262
<i>Bryoria fuscescens</i> (Gyeln.) Brodo & D. Hawksw.	S56	Velmala et al., 2014	GQ996291	KJ396502	GQ996263
<i>Bryoria fuscescens</i> (Gyeln.) Brodo & D. Hawksw.	L160	Velmala et al., 2014	GQ996300	KJ396497	GQ996272
<i>Bryoria fuscescens</i> (Gyeln.) Brodo & D. Hawksw.	S274	Velmala et al., 2014	GQ996303	KJ396512	GQ996276
<i>Bryoria fuscescens</i> (Gyeln.) Brodo & D. Hawksw.	L232	Velmala et al., 2014	GQ996304	KJ396500	GQ996277
<i>Bryoria fuscescens</i> (Gyeln.) Brodo & D. Hawksw.	L189	Velmala et al., 2014	GQ996305	KJ396498	GQ996278
<i>Bryoria fuscescens</i> (Gyeln.) Brodo & D. Hawksw.	S157	Velmala et al., 2014	GQ996306	KJ396504	GQ996279

<i>Bryoria fuscescens</i> (Gyeln.) Brodo & D. Hawksw.	S256	Velmala et al., 2014	GQ996307	KJ396505	GQ996280
<i>Bryoria fuscescens</i> (Gyeln.) Brodo & D. Hawksw.	L139	Velmala et al., 2014	KJ396436	KJ396495	KJ954309
<i>Bryoria fuscescens</i> (Gyeln.) Brodo & D. Hawksw.	L224	Velmala et al., 2014	KJ396437	KJ396499	KJ954310
<i>Bryoria fuscescens</i> (Gyeln.) Brodo & D. Hawksw.	L305	Velmala et al., 2014	KJ396438	–	–
<i>Bryoria fuscescens</i> (Gyeln.) Brodo & D. Hawksw.	L307	Velmala et al., 2014	KJ396439	–	KJ954311
<i>Bryoria fuscescens</i> (Gyeln.) Brodo & D. Hawksw.	S109	Velmala et al., 2014	KJ396440	KJ396503	KJ954312
<i>Bryoria fuscescens</i> (Gyeln.) Brodo & D. Hawksw.	S259	Velmala et al., 2014	KJ396441	KJ396506	KJ954313
<i>Bryoria fuscescens</i> (Gyeln.) Brodo & D. Hawksw.	S260a	Velmala et al., 2014	KJ396442	KJ396507	KJ954314
<i>Bryoria fuscescens</i> (Gyeln.) Brodo & D. Hawksw.	S261	Velmala et al., 2014	KJ396443	KJ396509	KJ954315
<i>Bryoria fuscescens</i> (Gyeln.) Brodo & D. Hawksw.	S369	Velmala et al., 2014	KJ396444	KJ396514	KJ954316
<i>Bryoria fuscescens</i> (Gyeln.) Brodo & D. Hawksw.	S379	Velmala et al., 2014	KJ396445	KJ396515	KJ954317
<i>Bryoria fuscescens</i> (Gyeln.) Brodo & D. Hawksw.	S380	Velmala et al., 2014	KJ396446	KJ396516	KJ954318
<i>Bryoria fuscescens</i> (Gyeln.) Brodo & D. Hawksw.	S24	Velmala et al., 2014	KJ576715	KJ396501	KJ599468
<i>Bryoria fuscescens</i> (Gyeln.) Brodo & D. Hawksw.	S267	Velmala et al., 2014	KJ576716	KJ396510	KJ599469
<i>Bryoria fuscescens</i> (Gyeln.) Brodo & D. Hawksw.	S272	Velmala et al., 2014	KJ576717	KJ396511	KJ599470
<i>Bryoria fuscescens</i> (Gyeln.) Brodo & D. Hawksw.	S277a	Velmala et al., 2014	KJ576718	KJ396513	KJ599471
<i>Bryoria glabra</i> (Motyka) Brodo & D. Hawksw.	L186	Velmala et al., 2014	FJ668494	FJ668456	FJ668400
<i>Bryoria implexa</i> (Hoffmann) Brodo & D. Hawksw	S22	Velmala et al., 2014	GQ996294	KJ396517	GQ996266

<i>Bryoria implexa</i> (Hoffmann) Brodo & D. Hawksw	S67	Velmala et al., 2014	KJ396447	KJ396520	KJ954319
<i>Bryoria implexa</i> (Hoffmann) Brodo & D. Hawksw	S168	Velmala et al., 2014	KJ396448	KJ396521	KJ954320
<i>Bryoria implexa</i> (Hoffmann) Brodo & D. Hawksw	S36	Velmala et al., 2014	KJ576719	KJ396518	KJ599472
<i>Bryoria implexa</i> (Hoffmann) Brodo & D. Hawksw.	S39	Velmala et al., 2014	GQ996293	KJ396519	GQ996265
<i>Bryoria inactiva</i> Goward, Velmala, & Myllys	L206	Velmala et al., 2014	GQ996283	KJ396522	GQ996255
<i>Bryoria inactiva</i> Goward, Velmala, & Myllys	S239a	Velmala et al., 2014	GQ996284	KJ396526	GQ996256
<i>Bryoria inactiva</i> Goward, Velmala, & Myllys	L323b	Velmala et al., 2014	KJ396449	KJ396523	KJ954321
<i>Bryoria inactiva</i> Goward, Velmala, & Myllys	L347	Velmala et al., 2014	KJ396450	KJ396524	KJ954322
<i>Bryoria inactiva</i> Goward, Velmala, & Myllys	L358	Velmala et al., 2014	KJ396451	KJ396525	KJ954323
<i>Bryoria inactiva</i> Goward, Velmala, & Myllys	S392a	Velmala et al., 2014	KJ396452	KJ396528	KJ954324
<i>Bryoria kockiana</i> Velmala, Myllys & Goward	L394	Velmala et al., 2014	KJ396453	KJ396529	KJ954325
<i>Bryoria kockiana</i> Velmala, Myllys & Goward	L396	Velmala et al., 2014	KJ396454	KJ396530	KJ954326
<i>Bryoria kuemmerleana</i> (Gyeln.) Brodo & D. Hawksw.	L244a	Velmala et al., 2014	GQ996295	KJ396531	GQ996267
<i>Bryoria kuemmerleana</i> (Gyeln.) Brodo & D. Hawksw.	L274	Velmala et al., 2014	GQ996296	KJ396532	GQ996268
<i>Bryoria kuemmerleana</i> (Gyeln.) Brodo & D. Hawksw.	L275	Velmala et al., 2014	KJ396455	KJ396533	KJ954327
<i>Bryoria kuemmerleana</i> (Gyeln.) Brodo & D. Hawksw.	S160	Velmala et al., 2014	KJ396456	KJ396535	KJ954328
<i>Bryoria kuemmerleana</i>	S128	Velmala et al., 2014	KJ576720	KJ396534	KJ599473

(Gyeln.) Brodo & D. Hawksw.					
<i>Bryoria pikei</i> Brodo & D. Hawksw.	L209	Velmala et al., 2014	GQ996281	KJ396538	GQ996253
<i>Bryoria pikei</i> Brodo & D. Hawksw.	L197	Velmala et al., 2014	KJ396457	KJ396536	KJ954329
<i>Bryoria pikei</i> Brodo & D. Hawksw.	L200	Velmala et al., 2014	KJ396458	KJ396537	KJ954330
<i>Bryoria pikei</i> Brodo & D. Hawksw.	L374	Velmala et al., 2014	KJ396459	KJ396540	KJ954331
<i>Bryoria pikei</i> Brodo & D. Hawksw.	L376	Velmala et al., 2014	KJ396460	KJ396541	KJ954332
<i>Bryoria pikei</i> Brodo & D. Hawksw.	L377	Velmala et al., 2014	KJ396461	KJ396542	KJ954333
<i>Bryoria pikei</i> Brodo & D. Hawksw.	L421	Velmala et al., 2014	KJ396462	KJ396543	KJ954334
<i>Bryoria pikei</i> Brodo & D. Hawksw.	S221	Velmala et al., 2014	KJ396463	KJ396544	KJ954335
<i>Bryoria pikei</i> Brodo & D. Hawksw.	S362	Velmala et al., 2014	KJ396464	KJ396545	KJ954336
<i>Bryoria pikei</i> Brodo & D. Hawksw.	S368	Velmala et al., 2014	KJ396465	KJ396546	KJ954337
<i>Bryoria pikei</i> Brodo & D. Hawksw.	S382	Velmala et al., 2014	KJ396466	KJ396547	KJ954338
<i>Bryoria pikei</i> Brodo & D. Hawksw.	S383a	Velmala et al., 2014	KJ396467	KJ396548	KJ954339
<i>Bryoria pikei</i> Brodo & D. Hawksw.	S390	Velmala et al., 2014	KJ396468	KJ396549	KJ954340
<i>Bryoria pikei</i> Brodo & D. Hawksw.	L210	Velmala et al., 2014	KJ576714	KJ396539	KJ599467
<i>Bryoria pikei</i> Brodo & D. Hawksw.	S394	Velmala et al., 2014	KJ576727	KJ396550	KJ599480
<i>Bryoria pseudofuscescens</i> (Gyeln.) Brodo & D. Hawksw.	S222	Velmala et al., 2014	KJ396469	KJ396551	KJ954341
<i>Bryoria pseudofuscescens</i> (Gyeln.) Brodo & D. Hawksw.	S232	Velmala et al., 2014	KJ396470	KJ396552	KJ954342
<i>Bryoria pseudofuscescens</i> (Gyeln.) Brodo & D. Hawksw.	S370	Velmala et al., 2014	KJ396471	KJ396553	KJ954343
<i>Bryoria pseudofuscescens</i> (Gyeln.) Brodo & D. Hawksw.	S371	Velmala et al., 2014	KJ396472	KJ396554	KJ954344
<i>Bryoria pseudofuscescens</i> (Gyeln.) Brodo & D. Hawksw.	S377	Velmala et al., 2014	KJ396473	KJ396555	KJ954345

<i>Bryoria pseudofuscescens</i> (Gyeln.) Brodo & D. Hawksw.	S386	Velmala et al., 2014	KJ576725	KJ396556	KJ599478
<i>Bryoria pseudofuscescens</i> (Gyeln.) Brodo & D. Hawksw.	S387	Velmala et al., 2014	KJ576726	KJ396557	KJ599477
<i>Bryoria vrangiana</i> (Gyeln.) Brodo & D. Hawksw.	S164	Velmala et al., 2014	GQ996285	KJ396574	GQ996257
<i>Bryoria vrangiana</i> (Gyeln.) Brodo & D. Hawksw.	S10	Velmala et al., 2014	GQ996297	KJ396564	GQ996269
<i>Bryoria vrangiana</i> (Gyeln.) Brodo & D. Hawksw.	S32	Velmala et al., 2014	GQ996298	KJ396565	GQ996270
<i>Bryoria vrangiana</i> (Gyeln.) Brodo & D. Hawksw.	L272	Velmala et al., 2014	GQ996299	KJ396558	GQ996271
<i>Bryoria vrangiana</i> (Gyeln.) Brodo & D. Hawksw.	L300	Velmala et al., 2014	GQ996301	KJ396562	GQ996274
<i>Bryoria vrangiana</i> (Gyeln.) Brodo & D. Hawksw.	S45	Velmala et al., 2014	GQ996302	KJ396568	GQ996275
<i>Bryoria vrangiana</i> (Gyeln.) Brodo & D. Hawksw.	S166	Velmala et al., 2014	GQ996308	KJ396575	GQ996273
<i>Bryoria vrangiana</i> (Gyeln.) Brodo & D. Hawksw.	L273	Velmala et al., 2014	KJ396474	KJ396559	KJ954346
<i>Bryoria vrangiana</i> (Gyeln.) Brodo & D. Hawksw.	L279	Velmala et al., 2014	KJ396475	KJ396560	KJ954347
<i>Bryoria vrangiana</i> (Gyeln.) Brodo & D. Hawksw.	L286	Velmala et al., 2014	KJ396476	KJ396561	KJ954348
<i>Bryoria vrangiana</i> (Gyeln.) Brodo & D. Hawksw.	S6	Velmala et al., 2014	KJ396477	KJ396563	KJ954349
<i>Bryoria vrangiana</i> (Gyeln.) Brodo & D. Hawksw.	S42	Velmala et al., 2014	KJ396478	KJ396566	KJ954350
<i>Bryoria vrangiana</i> (Gyeln.) Brodo & D. Hawksw.	S43	Velmala et al., 2014	KJ396479	KJ396567	KJ954351
<i>Bryoria vrangiana</i> (Gyeln.) Brodo & D. Hawksw.	S59	Velmala et al., 2014	KJ396480	KJ396571	KJ954352
<i>Bryoria vrangiana</i> (Gyeln.) Brodo & D. Hawksw.	S72	Velmala et al., 2014	KJ396481	KJ396573	KJ954353
<i>Bryoria vrangiana</i>	S196	Velmala et al., 2014	KJ396482	KJ396576	KJ954354

(Gyeln.) Brodo & D. Hawksw.					
<i>Bryoria vrangiana</i> (Gyeln.) Brodo & D. Hawksw.	S341b	Velmala et al., 2014	KJ396483	KJ396577	KJ954355
<i>Bryoria vrangiana</i> (Gyeln.) Brodo & D. Hawksw.	S385	Velmala et al., 2014	KJ396484	KJ396578	KJ954356
<i>Bryoria vrangiana</i> (Gyeln.) Brodo & D. Hawksw.	S62	Velmala et al., 2014	KJ576721	KJ396572	KJ599474
<i>Bryoria vrangiana</i> (Gyeln.) Brodo & D. Hawksw.	S57	Velmala et al., 2014	KJ576722	KJ396570	KJ599475
<i>Bryoria vrangiana</i> (Gyeln.) Brodo & D. Hawksw.	S47	Velmala et al., 2014	KJ576723	KJ396569	KJ599476
<i>Bryoria vrangiana</i> (Gyeln.) Brodo & D. Hawksw.	S396	Velmala et al., 2014	KJ576729	KJ396579	KJ599482
<i>Bryoria</i> sp.	L392	Velmala et al., 2014	KJ396485	KJ396580	KJ954357
<i>Bryoria</i> sp.	L395	Velmala et al., 2014	KJ396486	KJ396581	KJ954358

Table 5 Best partitioning scheme for each locus in the concatenated *Athelia* alignment. Results of the *Athelia* gene partitioning scheme and model selection indicate that ITS and each codon of EF1- α should run with separate evolutionary models during the maximum likelihood tree search..

Selection parameters – Branch lengths: linked; Models: GTR, GTR+G, GTR_I_G; Model Selection: AICc; Search: user defined. Scheme: all_separate; Scheme lnL: -7994.59130859375; Scheme AICc: 16470.161797; Parameters: 212; Sites: 1798; Subsets: 4; Scheme_all_separate (ITS) (EF1a_1) (EF1a_2) (EF1a_3).

Subset	Best Model	# sites	subset id	Partition names
1	GTR+G	715	10f75124a16cf7d37c17fe8956bcfcf7	ITS
2	GTR+G	361	b187892c48de77297196ce6c9038c24f	EF1a_1
3	GTR+G	361	97a7a71dc9d02763592bcb81a2dbfac9	EF1a_2
4	GTR+G	361	40f0c33692ebd309f12d1f77fad3cdc3	EF1a_3

Table 6 Best partitioning scheme for each locus in the concatenated *Bryoria* sect. *Implexae* alignment. Results of the *Bryoria* sect. *Implexae* gene partitioning scheme and model selection show that ITS, IGS, and each codon of GAPDH should run with separate evolutionary models during the maximum likelihood tree search.

Selection parameters – Branch lengths: linked; Models: GTR, GTR+G, GTR_I_G; Model Selection: AICc; Search: user defined. Scheme: all_separate; Scheme lnL: -4533.428771972656; Scheme AICc: 9833.5784879; Parameters: 322; Sites: 2018; Subsets: 5; Scheme_all_separate (ITS) (IGS) (GAPDH_1) (GAPDH_2) (GAPDH_3).

Subset	Best Model	# sites	subset id	Partition names
1	GTR+G	543	07eb0ebcb45476a9ba30b7a0227ebc21	ITS
2	GTR+G	421	e00bfb2dbbbeb0272d05757e5ecdd01c	IGS
3	GTR+G	352	e7fb4407e52cdf0ad0e4f50a945adde7	GAPDH_1
4	GTR	351	f81b7afb4a378d97cb7fbfea865e5574	GAPDH_2
5	GTR	351	0da36c06d84bdad41286d26d2fa6cc4b	GAPDH_3

Table 7 Approximately Unbiased (AU) test results suggest substrate preference does not explain evolutionary relationships across.

Constr.: constrained tree.

deltaL : logL difference from the maximal logL in the set.

p-AU : p-value of approximately unbiased (AU) test (Shimodaira, 2002).

Plus signs denote the 95% confidence sets.

Minus signs denote significant exclusion.

All tests performed 10000 resamplings using the RELL method.

Tree	logL	deltaL	p-AU
Tree 1: unconstrained (original) concatenated <i>Athelia</i> ML tree	-8048.089	0	0.9798+
Constr. 1: <i>Athelia</i> associated with epiphytic lichens are reciprocally monophyletic	-8746.805	698.716	0.0027-
Constr. 2: <i>Athelia</i> associated with fallen lichens are reciprocally monophyletic	-8760.701	712.613	0.0304-
Constr. 3: <i>Athelia</i> associated with wood or soil are reciprocally monophyletic	-8775.245	727.156	0-

Table 8 Average pairwise distance of ITS sequences between and within-strata of *Athelia* species/ group haplotypes. Results suggest greater nucleotide variation across members of *Athelia* than within *Athelia seborrheica*.

WITHIN		
<i>stratum</i>	<i>mean</i>	
acrospora	0.04131185	
arachnoidea	0.04810127	
Group I	0.03066104	
Group II	0.01821378	
seborrhea	0.02000817	
BETWEEN		
<i>strata.1</i>	<i>strata.2</i>	<i>mean</i>
acrospora	arachnoidea	0.04856157
acrospora	Group I	0.03607595
acrospora	Group II	0.0344649
acrospora	seborrheica	0.03525065
arachnoidea	Group I	0.05518987
arachnoidea	Group II	0.04189873
arachnoidea	seborrheica	0.04392801
Group I	Group II	0.03753165
Group I	seborrheica	0.03748022
Group II	seborrheica	0.01863133

Table 9 Average pairwise distance of EFI- α sequences between and within-strata of *Athelia* species/ group haplotypes. Results suggest greater nucleotide variation across members of *Athelia* than within *Athelia seborrheica*.

WITHIN		
<i>stratum</i>	<i>mean</i>	
Group I	0.13035382	
Group II	0.03910615	
seborrheica	0.01912801	
BETWEEN		
<i>strata.1</i>	<i>strata.2</i>	<i>mean</i>
Group I	Group II	0.12274984
Group I	seborrheica	0.07159761
Group II	seborrheica	0.08715472

Table 10 Results from the one-way analysis of variance (ANOVA) of morphological measurements between different species of *Athelia*. There are significant differences between basidia length and width, sterigmata length and width, and basidiospore length and width, but not in hyphal diameter for the species measured. Significant P-values are bolded and indicated by ***.

basidium.width~species_group					
	Df	Sum_Sq	Mean_Sq	F_value	Pr(>F)
species_group	3	53.39	17.798	44.17	<2e-16***
Residuals	326	131.34	0.403		

spore.width~species_group					
	Df	Sum_Sq	Mean_Sq	F_value	Pr(>F)
species_group	3	22.27	7.425	26.14	3.56e-15***
Residuals	326	92.61	0.284		

sterigmata.width~species_group					
	Df	Sum_Sq	Mean_Sq	F_value	Pr(>F)
species_group	3	0.55	0.1817	1.689	0.169
Residuals	325	34.96	0.1076		

hyphal.diameter~species_group					
	Df	Sum_Sq	Mean_Sq	F_value	Pr(>F)
species_group	3	8.53	2.8437	7.518	7.11e-05***
Residuals	316	119.53	0.3782		

basidium.length~species_group					
	Df	Sum_Sq	Mean_Sq	F_value	Pr(>F)
species_group	3	1357	452.4	76.28	<2e-16***
Residuals	326	1934	5.9		

spore.length~species_group					
	Df	Sum_Sq	Mean_Sq	F_value	Pr(>F)
species_group	3	38.91	12.97	20.32	4.28e-12***
Residuals	326	208.11	0.638		

sterigmata.length~species_group					
	Df	Sum_Sq	Mean_Sq	F_value	Pr(>F)
species_group	3	135.5	45.16	26.45	2.45e-15***
Residuals	326	556.6	1.71		

Table 11 Identity and frequency count of lichen hosts infected by *Athelia*. The genus *Bryoria* appears to be the preferential host genus, with species in *Bryoria* section *Implexae* most frequently encountered out of all macrolichens surveyed. All belong to the family Parmeliaceae.

Lichen Host	Specimen Count
<i>Bryoria</i> sect. <i>Implexae</i> (Gyeln.) Brodo & D. Hawksw.	42
<i>Bryoria fremontii</i> (Tuck.) Brodo & D.	3
<i>Bryoria tortuosa</i> (G. Merr.) Brodo & D. Hawksw.	1
<i>Bryoria simplicior</i> (Vain.) Brodo & D. Hawksw.	1
<i>Bryoria</i> sp. Brodo & D. Hawks.	8
<i>Alectoria sarmentosa</i> (Ach.) Ach.	5
<i>Nodobryoria abbreviata</i> (Müll. Arg.) Common & Brodo	1
<i>Nodobryoria oregana</i> (Tuck. ex Nyl.) Common & Brodo	2
<i>Usnea</i> spp.	16
<i>Evernia mesomorpha</i> Nyl.	3
<i>Hypogymnia physodes</i> (L.) Nyl.	4
<i>Platismatia glauca</i> (L.) W.L. Culb. & C.F. Culb.	2

Table 12 Voucher information for *Bryoria* sect. *Implexae* (Gyeln.) Brodo and D. Hawksw. collected and sequenced for this study. Final GenBank accession numbers for ITS, IGS, and GAPDH will be obtained upon formal submission of the publication. Successfully sequenced loci are indicated with an "x".

<u>Genus species</u>	<u>Extraction number</u>	<u>Locality</u>	<u>Elevation (m)</u>	<u>Collection number</u>	<u>Latitude</u>	<u>Longitude</u>	<u>ITS</u>	<u>IGS</u>	<u>GAPDH</u>
<i>Bryoria</i> sect. <i>Implexae</i>	SG357	Trophy Mountain, British Columbia, 9 Jun 2018	1802	S Goyette 525	51°45.611'N	119°56.287'W		x	x
<i>Bryoria</i> sect. <i>Implexae</i> (<i>pikai</i>)	SG410	~1-1.5 km from HWY to Fort McMurray (backroad), Alberta, 20 Apr 2018	592	S Goyette 299	55°23.596'N	112°28.396'W		x	x
<i>Bryoria</i> sect. <i>Implexae</i> (<i>subcana</i>)	SG414	outside Nojack, Alberta, 9 May 2018	821	S Goyette 393	53°35.070'N	115°37.341'W		x	x
<i>Bryoria</i> sect. <i>Implexae</i> (<i>capillaris</i>)	SG426	Athabasca County, Alberta, 4 Jun 2018	539	S Goyette 522	54°57.056'N	112°57.280'W		x	x
<i>Bryoria</i> sect. <i>Implexae</i>	SG436.1	Marten Lakes Wilderness Campus, Alberta, 23 Sep 2018	800	S Goyette 583	55°36'35.0"N	114°33'35.0"W	x	x	x
<i>Bryoria</i> sect. <i>Implexae</i> (<i>capillaris</i>)	SG441	Marten Lakes Wilderness Campus, Alberta, 22 Sep 2018	800	S Goyette 581	55°36'36.5"N	114°34'11.6"W		x	

Bryoria sect. Implexae (subcana)	SG441.2	Marten Lakes Wilderness Campus, Alberta, 22 Sep 2018	800	S Goyette 581	55°36'36.5"N	114°34'11.6"W		x	
<i>Bryoria sect. Implexae (fuscescens)</i>	SG450	off HWY 43 before Whitecourt, Alberta, 10 Jul 2018	700	S Goyette 536	54°06'16.5"N	115°37'39.0"W		x	x
<i>Bryoria sect. Implexae (fuscescens)</i>	SG455.1	outside Chinook Cove, British Columbia	760	T Spribille	51°15'31.2"N	120°12'44.7"W		x	x
<i>Bryoria sect. Implexae (capillaris)</i>	SG455.2	outside Chinook Cove, British Columbia	760	T Spribille	51°15'31.2"N	120°12'44.7"W		x	x
<i>Bryoria sect. Implexae (capillaris)</i>	SG456.2	past Falkland, British Columbia	810	T Spribille	50°26'08.4"N	119°30'17.7"W		x	x
<i>Bryoria sect. Implexae (sorediate)</i>	SG458.1	past Falkland, British Columbia	810	T Spribille	50°26'08.4"N	119°30'17.7"W		x	x
<i>Bryoria sect. Implexae (fuscescens)</i>	SG458.3	past Falkland, British Columbia	810	T Spribille	50°26'08.4"N	119°30'17.7"W	x	x	x
<i>Bryoria sect. Implexae (capillaris)</i>	SG458.4	past Falkland, British Columbia	810	T Spribille	50°26'08.4"N	119°30'17.7"W	x	x	x
<i>Bryoria sect. Implexae (fuscescens)</i>	SG459.1	outside Chinook Cove, British Columbia	760	T Spribille	51°15'31.2"N	120°12'44.7"W	x	x	x
<i>Bryoria sect. Implexae (sorediate)</i>	SG459.2	outside Chinook Cove, British Columbia	760	T Spribille	51°15'31.2"N	120°12'44.7"W	x	x	x
<i>Bryoria sect. Implexae (capillaris)</i>	SG459.3	outside Chinook Cove, British Columbia	760	T Spribille	51°15'31.2"N	120°12'44.7"W	x	x	x

<i>Bryoria sect. Implexae (fuscescens)</i>	SG460.1	past Falkland, British Columbia	760	T Spribille	51°15'31.2"N	120°12'44.7"W	x	x	x
<i>Bryoria sect. Implexae (capillaris)</i>	SG460.2	past Falkland, British Columbia	810	T Spribille	51°15'31.2"N	120°12'44.7"W		x	x
<i>Bryoria sect. Implexae</i>	SG461.2	outside Chinook Cove, British Columbia	810	T Spribille	50°26'08.4"N	119°30'17.7"W	x	x	x
<i>Bryoria sect. Implexae (fuscescens)</i>	SG498.2	outside of Lolo Pass, Idaho	1280	S Goyette 626	46°47'05.7"N	114°23'02.1"W	x	x	x
<i>Bryoria sect. Implexae (fuscescens)</i>	SG507.2	outside Stryker, Montana, 6 Apr 2019	1211	S Goyette 629	48°41.510'N	114°44.173'W	x	x	x
<i>Bryoria sect. Implexae (capillaris)</i>	SG507.3	outside Stryker, Montana, 6 Apr 2019	1211	S Goyette 629	48°41.510'N	114°44.173'W	x	x	x
<i>Bryoria sect. Implexae (sorediate)</i>	SG510.1	outside of Stryker, Montana, 6 Apr 2019	1211	S Goyette 630	48°41.510'N	114°44.173'W	x	x	x
<i>Bryoria sect. Implexae (fuscescens)</i>	SG510.2	outside of Stryker, Montana, 6 Apr 2019	1211	S Goyette 630	48°41.510'N	114°44.173'W	x	x	
<i>Bryoria sect. Implexae</i>	SG512.1	Edna Creek Rd. area, Montana, 7 Apr 2019	1352	S Goyette 631	48°40.391'N	115°01.109'W		x	x
<i>Bryoria sect. Implexae</i>	SG521.2	outside Edna Creek Rd. area, Montana, 7 Apr 2019	446	T Spribille	48°40.391'N	115°01.109'W	x	x	x
<i>Bryoria sect. Implexae</i>	SG524.1	on <i>Abies lasiocarpa</i> , Edna Creek Rd. area, Montana, 7 Apr 2019	1352	S Goyette 633	48°40.391'N	115°01.109'W	x	x	x

<i>Bryoria sect. Implexae (capillaris)</i>	SG524.2	on <i>Abies lasiocarpa</i> , Edna Creek Rd. area, Montana, 7 Apr 2019	1352	S Goyette 633	48°40.391'N	115°01.109'W	x	x	x
<i>Bryoria sect. Implexae (sorediate)</i>	SG525.1	outside Edna Creek Rd. area, Montana, 6 Apr 2019	1211	S Goyette 634	48°41.510'N	114°44.173'W		x	x
<i>Bryoria sect. Implexae (fuscescens)</i>	SG525.2	outside Edna Creek Rd. area, Montana, 6 Apr 2019	1211	S Goyette 634	48°41.510'N	114°44.173'W		x	x
<i>Bryoria sect. Implexae (sorediate)</i>	SG527.1	Edna Creek Rd. area, Montana, 7 Apr 2019	1352	S Goyette 636	48°40.391'N	115°01.109'W	x	x	x
<i>Bryoria sect. Implexae (capillaris)</i>	SG527.2	Edna Creek Rd. area, Montana, 7 Apr 2019	1352	S Goyette 636	48°40.391'N	115°01.109'W	x	x	x
<i>Bryoria sect. Implexae (capillaris)</i>	SG528.1	Edna Creek Rd. area, Montana, 7 Apr 2019	1352	S Goyette 637	48°40.391'N	115°01.109'W	x	x	x
<i>Bryoria</i> sp.	SG542.2	Mukiki Lake, Alberta, 18 May 2019	1580	S Goyette 638	52°50.678'N	116°51.715'W	x	x	x
<i>Bryoria sect. Implexae</i>	SG548.1	Yellowhead County, Alberta, 18 May 2019	1935	S Goyette 639	52°53.110'N	116°58.891'W	x	x	x
<i>Bryoria</i> sp.	SG548.3	Yellowhead County, Alberta, 18 May 2019	1935	S Goyette 639	52°53.110'N	116°58.891'W	x	x	x
<i>Bryoria sect. Implexae</i>	SG558.2	Coquihalla Pass, British Columbia, 11 May 2019	1220	T Spribille	49°35'38.2"N	121°07'16.8"W	x		x
<i>Bryoria sect. Implexae</i>	SG567.1	Lily Lake Trail, Alberta, 25 May 2019	970	T Spribille	55°28'01.3"N	114°42'49.1"W		x	x

<i>Bryoria sect. Implexae (fuscescens)</i>	SG574.1	outside Stryker/ Stillwater, Montana, 6 Apr 2019	1211	S Goyette 645	48°41.510'N	114°44.173'W		x	x
<i>Bryoria sect. Implexae</i>	SG624.1	Uppland, Vänge parish, 5.5 km NW of Vänge village, 25 m W of the border to the nature reserve Fiby Urskog, Sweden	130	T Spribille	59°52'51.7"N	17°21'05.9"E		x	x
<i>Bryoria sect. Implexae (pikei)</i>	SG635.2	Little Lost Lake trail loop, British Columbia, 11 May 2019	800	S Goyette 646	55°36'36.5"N	114°34'11.6"W		x	x
<i>Bryoria glabra</i>	SG653.1	Philip Creek drainage: 1 km west of Philip Lake, Upper Clearwater Valley, British Columbia, 28 Aug 2019	1600	T. Goward 19-154	51°52'15.4"N	119°55'02.3"W		x	x
<i>Bryoria sect. Implexae</i>	SG656.1	26 km north of Clearwater Village: 1 km w of "Edgewood Blue", Upper Clearwater Valley, British Columbia, 28 Aug 2019	715	T. Goward 19-155	51°52'09.7"N	120°01'18.0"W		x	x

Table 13 Chemical and morphological data matrix for *Bryoria* sect. *Implexae* following Velmala et al. (2014). Isolates SG512.1 and SG521.2 did not have enough usable material for morphological character scoring or chemical analysis. Isolates SG436.1, SG441.2, SG455.2, SG525.1, and SG574.1 did not have enough usable material for chemical analysis. The "-" indicate that a given character was not present to be scored. For instance if the specimen lacked "pseudocyphellae" subsequent pseudocyphellae characters (color, surface, etc.) could not be included in the data matrix.

1 -orcinol depsidones: absent (0), present (1), see characters 2–4; 2 Fumarprotocetraric acid: absent (0), present only in soralia (1), present in thallus (2); 3 Norstictic acid: absent (0), present (1); 4 Psoromic acid: absent (0), present (1); 5 -orcinol depsides: absent (0), present (1), see characters 6–8; 6 Atranorin and/or chloroatranorin: absent (0), present (1); 7 Alectorialic acid: absent (0), present (1); 8 Barbatolic acid: absent (0), present (1); 9 Gyrophoric acid (= orcinol depside): absent (0), present (1); 10 Soralia: absent (0), present (1); 11 Pseudocyphellae: absent or very rare (0), present (1); 12 Pseudocyphellae color: brownish white (0), white (1); 13 Pseudocyphellae surface: slightly depressed or plane (0), partly raised (1); 14 Pseudocyphellae shape: linear (0), elongate-fusiform (1); 15 Thallus color: gray to pale brown (0), brown (1), dark brown to black (2); 16 Apothecia: absent (0), present (1); 17 Branching angles: mainly acute (0), mainly obtuse (1), both (2); 18 Origin: North America (0), Europe or Asia (1)

Isolate	Character																	
	1	2	3	4	5	6	7	8	9	10	11	12	13	14	15	16	17	18
L141	0	0	0	0	1	0	1	1	0	0	0	-	-	-	0	0	2	1
L211	1	1	0	0	1	0	1	1	0	1	0	-	-	-	0	0	0	1
L270	0	0	0	0	1	-	-	1	0	1	0	-	-	-	0	0	0	1
S2	0	0	0	0	1	0	1	1	0	1	0	-	-	-	0	0	0	1
S192	0	0	0	0	1	1	1	1	0	0	1	0	0	0	0	0	0	1
L355	0	0	0	0	0	0	0	0	1	0	1	0	0	0	2	0	2	0
L407	0	0	0	0	0	0	0	0	1	0	1	0	0	1	1	0	2	0
L395a	0	0	0	0	0	0	0	0	1	0	1	1	0	1	1	-	1	0
L147	1	2	0	0	0	0	0	0	0	1	0	-	-	-	2	0	0	1
L139	1	2	0	0	0	0	0	0	0	1	0	-	-	-	0	0	0	1
L149	1	2	0	0	0	0	0	0	0	1	0	-	-	-	1	0	0	1
L160	1	2	0	0	1	1	0	0	0	1	0	-	-	-	1	0	0	1
L189	1	2	0	0	0	0	0	0	0	1	0	-	-	-	0	0	0	1
L224	1	2	0	0	0	0	0	0	0	1	0	-	-	-	2	0	0	1
L232	1	1	0	0	1	1	0	0	0	1	0	-	-	-	2	0	2	1
S24	1	1	0	0	0	0	0	0	0	1	0	-	-	-	2	0	0	1
S56	1	2	0	0	0	0	0	0	0	1	0	-	-	-	2	0	0	1
S109	1	2	0	0	1	1	0	0	0	1	0	-	-	-	0	0	0	1
S157	1	2	0	0	1	1	0	0	0	1	0	-	-	-	1	0	2	1
S256	1	1	0	0	0	0	0	0	0	1	0	-	-	-	1	0	0	0
S259	1	1	0	0	0	0	0	0	0	1	0	-	-	-	2	0	0	0

S260a	1	1	0	0	0	0	0	0	0	1	0	-	-	-	2	0	0	0
S260b	1	1	0	0	0	0	0	0	0	1	0	-	-	-	2	0	0	0
S261	1	1	0	0	0	0	0	0	0	1	0	-	-	-	1	0	0	0
S267	1	1	0	0	0	0	0	0	0	1	0	-	-	-	1	0	0	0
S272	1	1	0	0	0	0	0	0	0	1	0	-	-	-	2	0	0	0
S274	0	0	0	0	0	0	0	0	0	1	0	-	-	-	2	0	0	0
S277a	1	1	0	0	0	0	0	0	0	1	0	-	-	-	2	0	0	0
S369	1	1	0	0	0	0	0	0	0	1	0	-	-	-	2	0	0	0
S379	1	1	0	0	0	0	0	0	0	1	0	-	-	-	2	0	0	0
S380	1	1	0	0	0	0	0	0	0	1	-	-	-	-	2	0	0	0
L186	1	1	0	0	0	0	0	0	0	1	0	-	-	-	1	0	2	1
S22	1	0	0	1	1	1	0	0	0	1	1	1	1	1	1	0	2	1
S36	1	0	0	1	0	0	0	0	0	0	1	1	0	1	0	0	0	1
S39	1	0	0	1	0	0	0	0	0	1	1	1	1	1	1	0	0	1
S67	1	0	0	1	1	1	0	0	0	0	1	1	1	1	1	0	2	1
S168	1	0	0	1	1	1	0	0	0	1	1	-	-	-	1	1	0	1
L206	0	0	0	0	0	0	0	0	0	0	1	0	0	1	1	0	0	0
L323b	0	0	0	0	0	0	0	0	0	0	1	1	0	0	1	0	2	0
L347	0	0	0	0	0	0	0	0	0	0	1	0	0	1	1	1	2	0
L358	0	0	0	0	0	0	0	0	0	0	1	0	0	0	1	0	2	0
S239a	0	0	0	0	0	0	0	0	0	0	1	0	0	0	1	0	2	0
S384	0	0	0	0	0	0	0	0	0	0	1	1	0	0	2	0	0	0
S392a	0	0	0	0	0	0	0	0	0	0	1	0	0	0	1	1	0	0
L394	1	0	0	1	1	1	0	0	0	0	1	1	1	1	0	0	0	0
L396	1	0	0	1	0	0	0	0	0	0	1	0	1	1	1	0	0	0
L244a	1	0	1	0	1	1	0	0	0	1	1	0	0	1	2	0	0	1
L274	1	0	1	0	1	1	0	0	0	1	1	0	1	1	1	0	1	1
L275	1	0	1	0	1	1	0	0	0	1	1	0	0	1	1	0	1	1
S128	1	0	1	0	1	1	1	0	0	0	1	1	0	0	1	0	2	1
S160	1	0	1	0	1	1	0	0	0	1	1	0	1	1	1	0	0	1
L197	0	0	0	0	1	0	1	1	0	0	1	0	0	1	1	1	0	0
L200	0	0	0	0	1	0	1	1	0	0	1	0	0	1	1	1	0	0
L209	0	0	0	0	1	0	1	1	0	0	1	0	0	1	1	1	0	0
L210	0	0	0	0	1	0	1	1	0	0	1	0	0	1	1	0	2	0
L374	0	0	0	0	1	0	1	0	1	0	1	0	0	1	2	0	0	0
L376	0	0	0	0	1	0	1	0	1	0	1	0	0	1	1	0	0	0
L377	0	0	0	0	1	0	1	0	1	0	1	1	0	1	0	1	2	0
L421	0	0	0	0	1	0	1	0	1	0	1	0	1	1	0	0	0	0
S221	0	0	0	0	1	0	1	1	0	0	1	0	0	1	0	0	0	0
S362	0	0	0	0	1	0	1	1	0	0	1	0	0	0	1	0	0	0

S368	0	0	0	0	1	0	1	1	0	0	1	0	0	1	1	1	0	0
S382	0	0	0	0	1	0	1	1	0	0	1	0	0	1	0	0	0	0
S383a	0	0	0	0	1	0	1	1	0	0	1	1	0	1	0	0	0	0
S390	0	0	0	0	1	0	1	1	0	0	1	-	-	-	1	0	0	0
S394	0	0	0	0	1	0	1	1	0	0	1	0	0	1	0	0	0	0
S222	1	0	1	0	0	0	0	0	0	0	1	1	1	1	1	0	0	0
S232	1	0	1	0	0	0	0	0	0	0	1	1	0	1	1	0	0	0
S370	1	0	1	0	0	0	0	0	0	0	1	1	0	1	1	0	0	0
S371	1	0	1	0	0	0	0	0	0	0	1	1	0	1	2	0	0	0
S377	1	0	1	0	0	0	0	0	0	0	1	1	0	0	2	0	0	0
S386	1	0	1	0	0	0	0	0	0	0	1	1	0	1	2	0	0	0
S387	1	0	1	0	0	0	0	0	0	0	1	1	0	1	2	1	2	0
L272	1	1	0	0	0	0	0	0	1	1	1	1	1	1	1	1	1	1
L273	1	1	0	0	0	0	0	0	0	1	1	0	0	1	1	0	2	1
L279	1	2	0	0	0	0	0	0	0	1	1	0	0	1	1	0	2	1
L286	1	2	0	0	1	1	0	0	0	1	1	0	0	1	1	1	1	1
L300	1	1	0	0	0	0	0	0	0	1	1	0	0	1	1	1	1	1
S6	1	2	0	0	0	0	0	0	0	1	1	0	0	1	1	0	0	1
S10	0	0	0	0	0	0	0	0	1	0	1	0	0	-	1	0	2	1
S32	1	1	0	0	1	1	0	0	1	1	1	0	0	1	2	0	0	1
S42	1	1	0	0	0	0	0	0	1	1	1	0	0	1	1	1	2	1
S43	1	1	0	0	0	0	0	0	1	1	1	0	0	1	1	0	2	1
S45	1	1	0	0	0	0	0	0	0	1	1	0	0	1	1	1	2	1
S47	1	1	0	0	0	0	0	0	0	1	1	0	0	1	1	1	0	1
S57	1	2	0	0	1	1	0	0	0	0	1	0	0	1	1	1	2	1
S59	1	1	0	0	1	1	0	0	0	1	1	0	0	1	1	0	2	1
S62	1	1	0	0	1	1	0	0	1	1	1	0	0	1	1	0	0	1
S72	1	1	0	0	0	0	0	0	0	1	1	0	0	0	2	0	1	1
S164	1	1	0	0	1	1	0	0	0	1	1	0	0	1	2	0	0	1
S166	1	2	0	0	1	1	0	0	0	1	1	0	0	1	1	0	0	1
S196	1	1	0	0	0	0	0	0	0	1	1	0	0	1	1	0	0	1
S341b	1	1	0	0	0	0	0	0	0	1	1	0	0	0	1	0	1	1
S385	1	1	0	0	0	0	0	0	0	1	1	0	0	0	1	0	2	0
S396	1	2	0	0	1	1	0	0	0	1	1	0	0	1	1	1	0	1
L392	0	0	0	0	0	0	0	0	0	0	1	0	0	1	1	0	0	0
L395	0	0	0	0	0	0	0	0	0	0	1	0	0	1	2	0	0	0
SG357	1	0	0	1	1	0	0	1	0	0	0	-	-	-	0	0	0	0
SG410	1	0	0	0	1	0	0	1	0	0	0	0	1	1	0	1	0	0
SG414	0	0	0	0	0	0	0	0	0	0	1	0	0	0	1	0	0	0
SG426	1	0	0	1	1	0	0	0	1	0	1	0	1	0	0	0	0	0

SG436.1										0	0	-	-	-	2	0	0	0
SG441	1	0	1	0	1	0	0	1	0	1	1	0	0	1	0	0	1	1
SG441.2										1	1	0	0	1	1	0	0	1
SG450	1	1	0	0	0	0	0	0	0	1	1	0	0	0	2	0	0	0
SG455.1	0	0	1	0	0	0	0	0	0	1	1	1	0	1	1	0	0	0
SG455.2										0	1	0	0	1	0	0	0	0
SG456.2	0	0	0	0	1	0	0	1	0	0	1	1	0	0	0	0	0	0
SG458.1	1	1	1	0	0	0	0	0	0	1	0	1	0	1	1	0	2	0
SG458.3	0	0	0	0	0	0	0	0	0	0	1	0	0	1	1	0	2	0
SG458.4	0	0	1	0	1	0	0	0	1	0	1	0	0	1	0	0	0	0
SG459.1	0	0	0	0	0	0	0	0	0	0	1	0	0	1	1	0	0	0
SG459.2	1	1	0	0	0	0	0	0	0	1	0	1	0	1	1	0	0	0
SG459.3	1	0	0	1	1	0	0	1	0	0	1	0	0	1	0	0	0	0
SG460.1	1	1	0	0	0	0	0	0	0	0	1	1	0	1	1	0	1	0
SG460.2	1	0	0	1	0	0	0	0	0	0	1	1	0	0	0	0	0	0
SG461.2	0	0	0	0	0	0	0	0	0	1	1	0	0	1	0	0	2	0
SG498.2	0	0	0	0	0	0	0	0	0	0	1	0	0	0	2	0	0	0
SG507.2	0	0	0	0	0	0	0	0	0	0	0	1	0	0	1	0	1	0
SG507.3	0	0	0	0	1	0	0	1	0	0	1	1	0	0	0	0	0	0
SG510.1	1	1	0	0	0	0	0	0	0	1	0	-	-	-	1	0	1	0
SG510.2	0	0	0	0	0	0	0	0	0	0	1	0	0	1	1	0	0	0
SG512.1																		0
SG521.2																		0
SG524.1	1	1	0	0	0	0	0	0	0	1	0	-	-	-	0	0	0	0
SG524.2	1	0	0	1	1	0	0	1	0	0	1	1	0	0	1	0	0	0
SG525.1										1	1	1	0	1	1	0	2	0
SG525.2	0	0	0	0	1	0	0	1	0	0	1	0	0	1	1	0	2	0
SG527.1	1	1	0	0	0	0	0	0	0	1	0	-	-	-	0	0	1	0
SG527.2	1	0	1	0	0	0	0	0	0	0	1	0	0	1	1	0	0	0
SG528.1	1	0	0	1	1	0	0	1	0	0	0	-	-	-	0	0	0	0
SG548.1	1	1	0	0	0	0	0	0	0	1	0	-	-	-	2	0	1	0
SG558.2	0	0	0	0	1	0	0	1	0	0	1	0	0	0	1	0	0	0
SG567.1	1	0	0	1	1	0	0	1	0	0	0	0	1	1	0	0	0	0
SG574.1										1	1	0	0	1	1	0	0	0
SG624.1	1	0	0	1	1	0	0	1	0	0	0	-	-	-	0	0	2	1
SG635.2	1	0	0	1	0	0	0	0	1	0	0	0	0	1	0	0	2	0
SG653.1	1	1	0	0	0	0	0	0	0	1	0	-	-	-	2	0	1	0
SG656.1	1	0	0	1	1	0	0	1	0	0	0	-	-	-	1	1	0	0

Table 14 Diagnostic characters for *Athelia* species most similar to *A. seborrheica*. *Athelia seborrheica* can be differentiated from *A. arachnoidea* in its shorter basidia and four sterigmata, from *A. acrospora* in its stouter basidiospores, and from *A. epiphylla* in its slightly longer though narrower basidia, wider basidiospores, and preferential infection of hair lichens in Parmeliaceae.

<u>Genus species</u>	<u>Basidium length x width (µm)</u>	<u>Sterigmata length x width (µm)</u>	<u>Sterigmata number</u>	<u>Basidiospore length x width width (µm)</u>	<u>Substrate</u>	<u>Reference</u>
<i>Athelia seborrheica</i>	14–18.5–(20) x 5.5–6–(7)	3.5–5.5 x 1–1.5	4, rarely 2	4.5–5.5 x 3–3.5–(4.5)	<i>Abies lasiocarpa</i> wood; Lichen: <i>Bryoria</i> sect. <i>Implexae</i> , <i>Bryoria fremontii</i> , <i>Bryoria tortuosa</i> , <i>Alectoria sarmentosa</i> , <i>Nodobryoria abbreviata</i> , <i>Nodobryoria oregana</i> , <i>Usnea spp.</i> , <i>Evernia mesomorpha</i> , <i>Hypogymnia physodes</i> , <i>Platismatia glauca</i>	This study
<i>Athelia acrospora</i>	12–15 x 5–6	3 x 8	4, rarely 2	5.5–7–(8) x 2.2–2.6	Gymnosperm and angiosperm wood; Angiosperm leaves	Jülich, 1972
<i>Athelia arachnoidea</i>	24–33 x 6.5–8	5–6 x 1.5–2	2, rarely 4	(7)–8–11–(12) x (3.5)–4–5.5–(6)	Gymnosperm and angiosperm wood; Lichen: <i>Lecanora spp.</i> , <i>Physcia ascendens</i> , <i>Xanthoria parietina</i> , <i>Usnea barbata</i>	Jülich, 1972
<i>Athelia epiphylla</i>	13–15–18 x 5–7–8	4–5 x 1	4, rarely 2	(5.5)–6–7.5–(8) x 2.8–3.2	Gymnosperm and angiosperm wood; various ferns; Moss: <i>Hylocomium splendens</i> ; Lichen: <i>Parmelia</i> , <i>Xanthoria</i>	Jülich, 1972

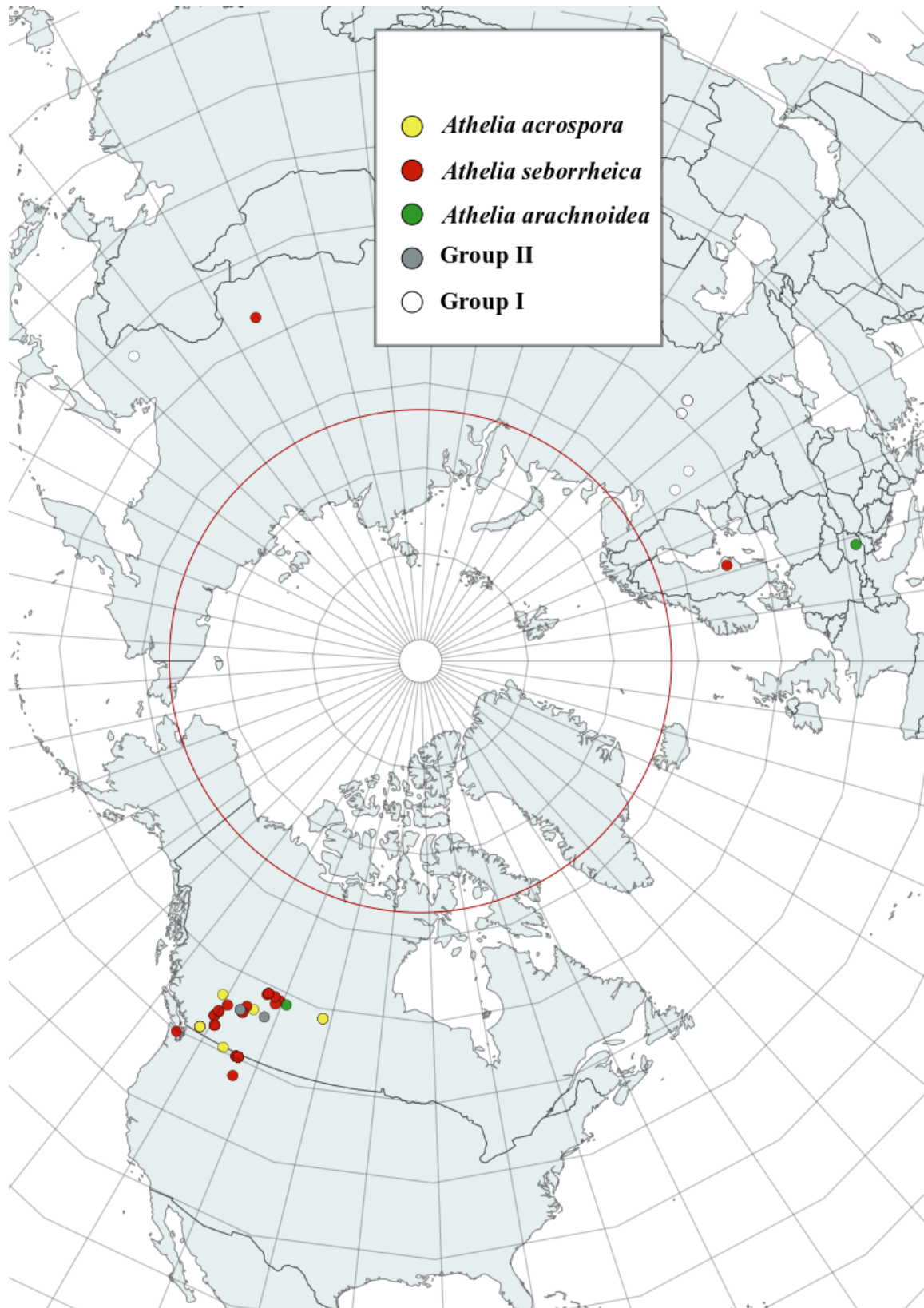


Figure 1 Map of *Athelia* collected and sequenced for this study, color-coded by species or group.

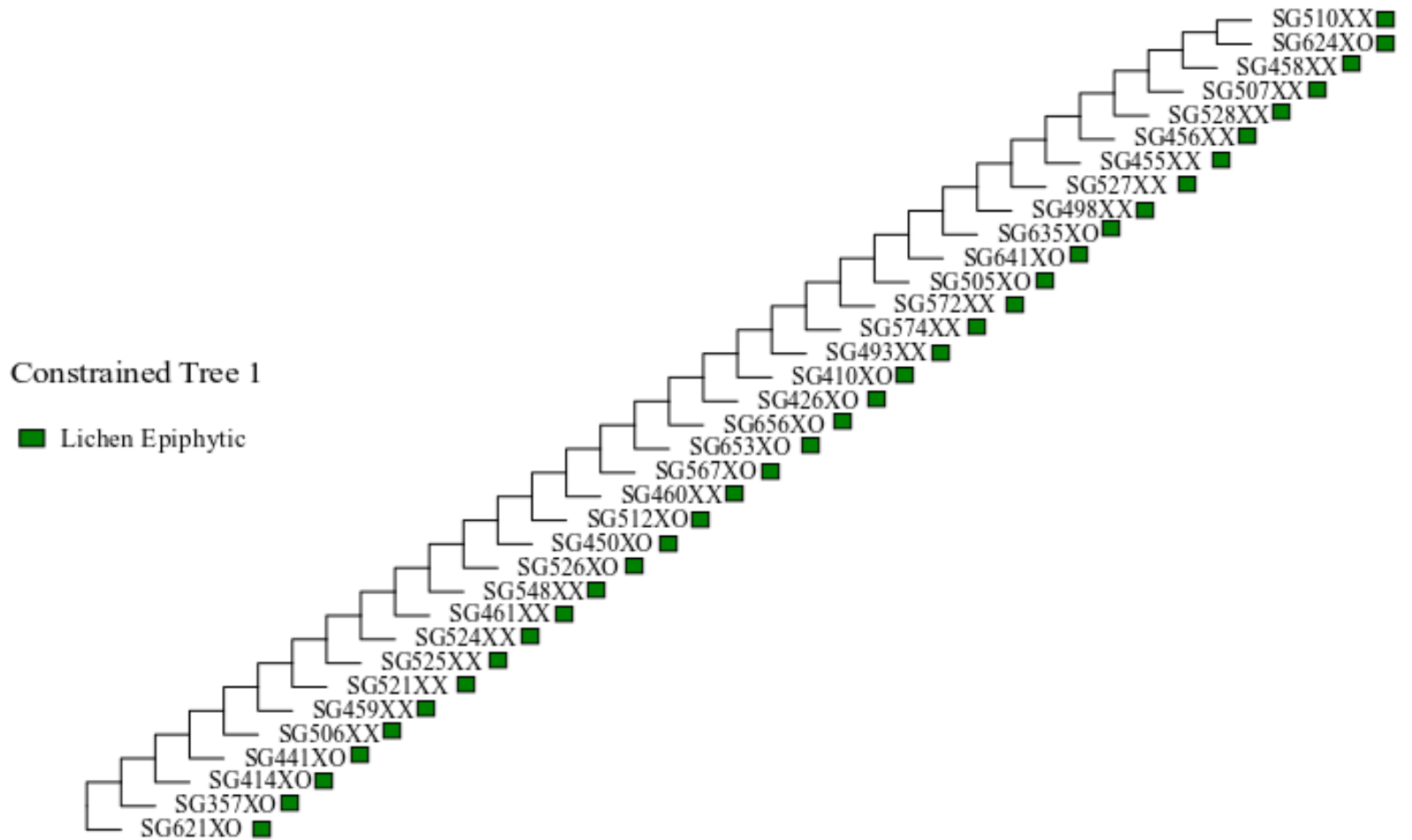


Figure 2 Constrained *Athelia* tree 1: *Athelia* from epiphytic lichen are monophyletic.

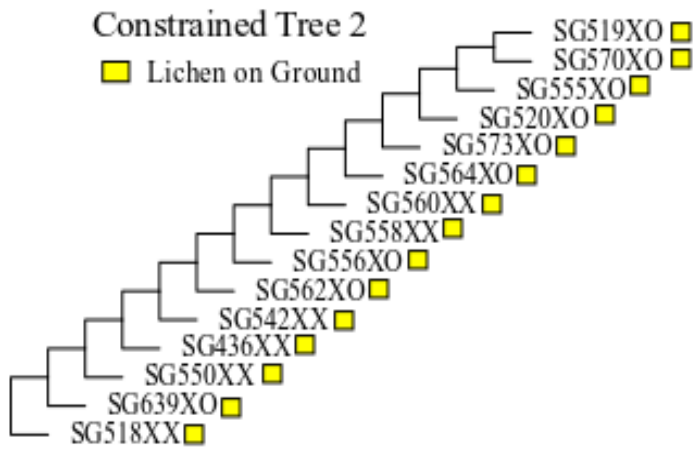


Figure 3 Constrained *Athelia* tree 2: *Athelia* from fallen lichen are monophyletic.

Constrained Tree 3

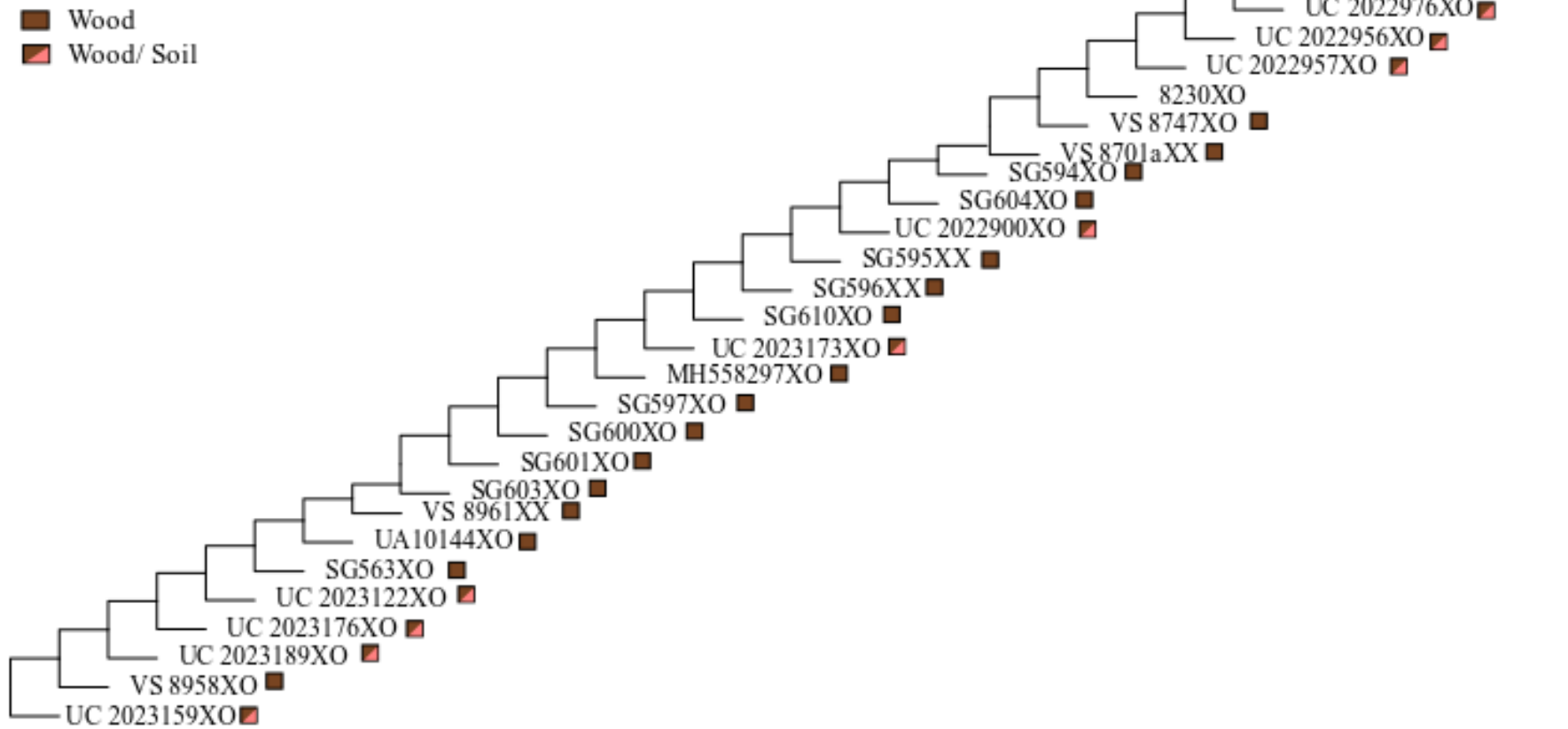
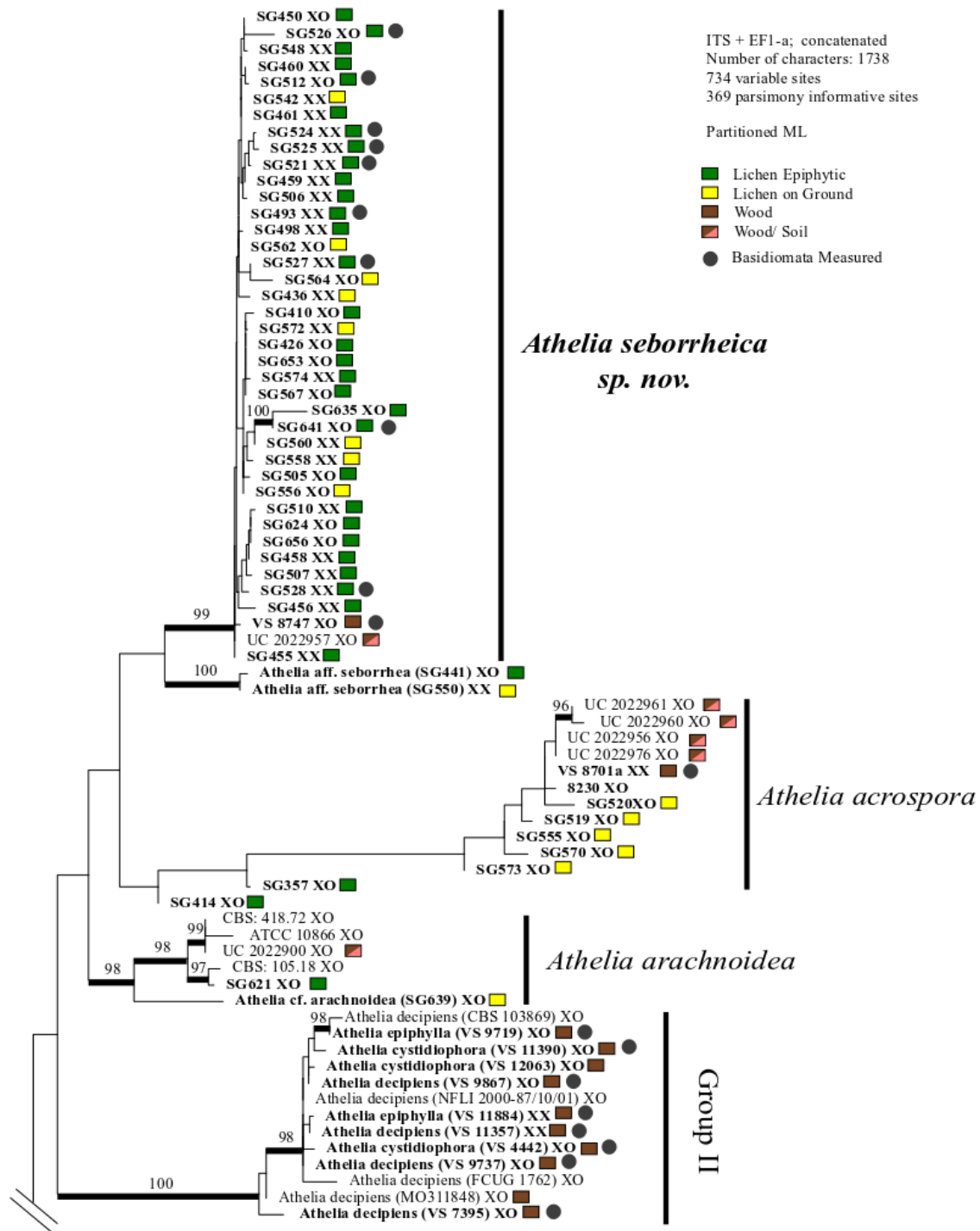


Figure 4 Constrained *Athelia* tree 3: *Athelia* from wood and soil are monophyletic.



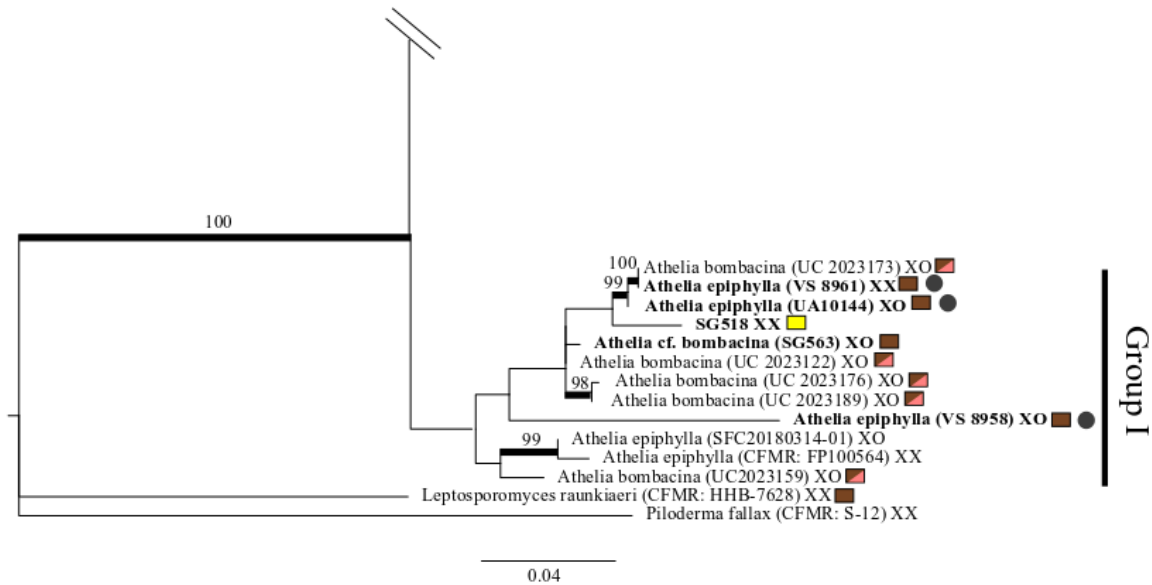
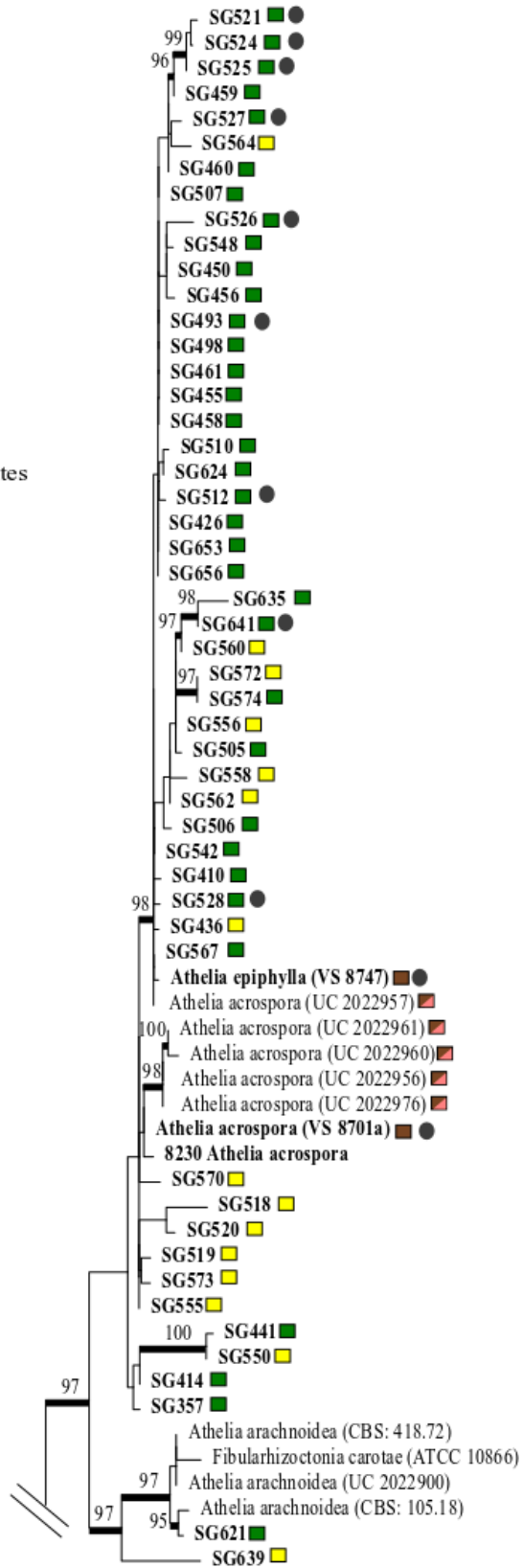


Figure 5 Concatenated ITS – *EFI- α* maximum likelihood (ML) *Athelia* tree. Branches with ultrafast bootstrapping support $\geq 95\%$ indicated with bolded bars. Bolded tips indicate sequences and specimens new to this study. **X** = a given locus was successfully sequenced or available on GenBank for a given specimen; **O** = a given locus was not successfully sequenced or available on GenBank for a given specimen. **SG** refers to Spencer Goyette's DNA isolate numbers, **VS** refers to Viacheslav Spirin collection numbers.

ITS
 Number of characters: 685
 349 variable sites
 135 parsimony informative sites

ML

- Lichen Epiphytic
- Lichen on Ground
- Wood
- Wood/ Soil
- Basidiomata Measured



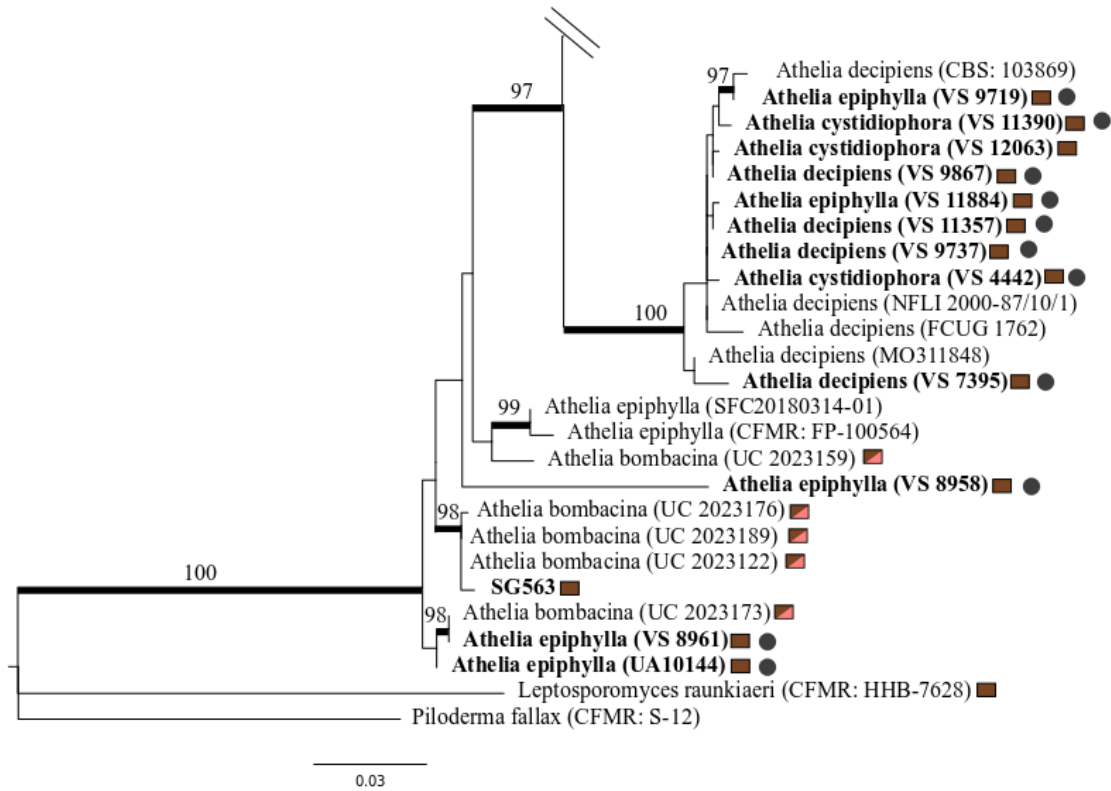


Figure 6 ITS maximum likelihood *Athelia* tree. Branches with ultrafast bootstrapping support $\geq 95\%$ indicated with bolded bars. Bolded tips indicate sequences and specimens new to this study. **SG** refers to Spencer Goyette's isolate numbers, **VS** refers to Viacheslav Spirin's collection numbers.

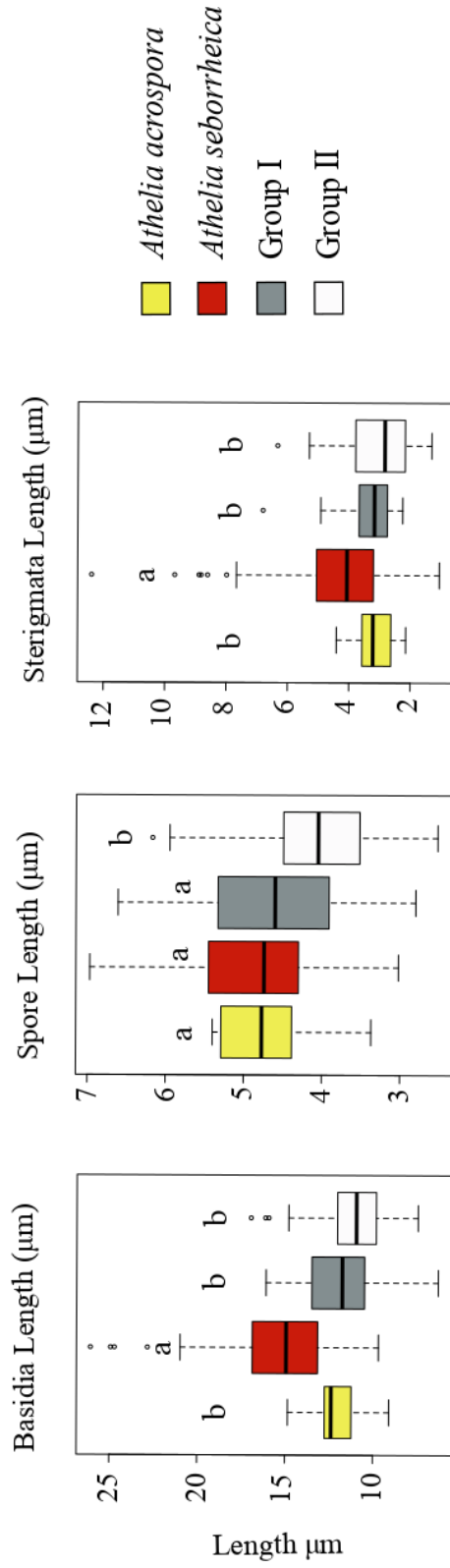
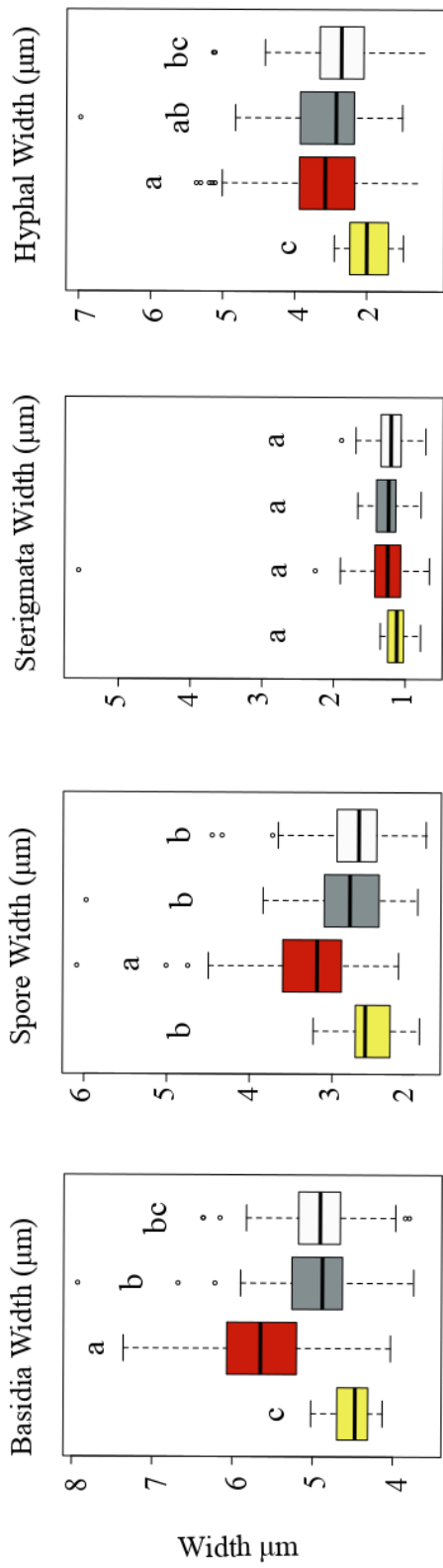
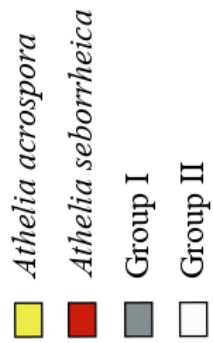
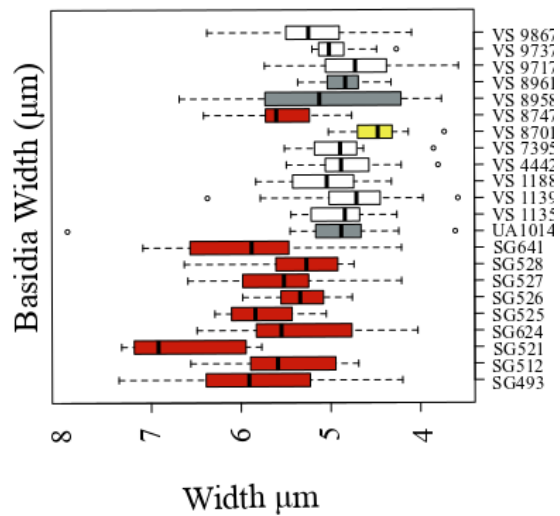
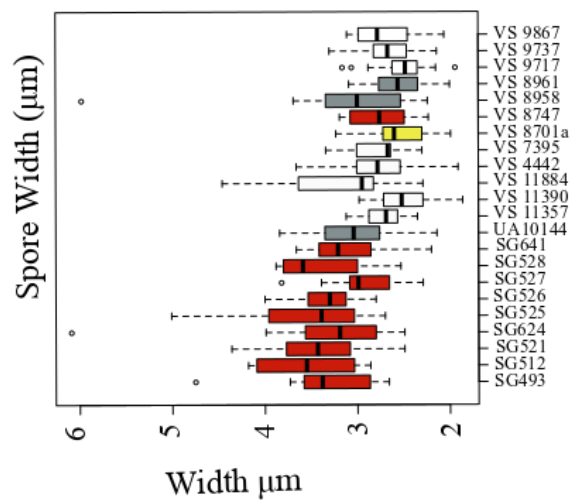
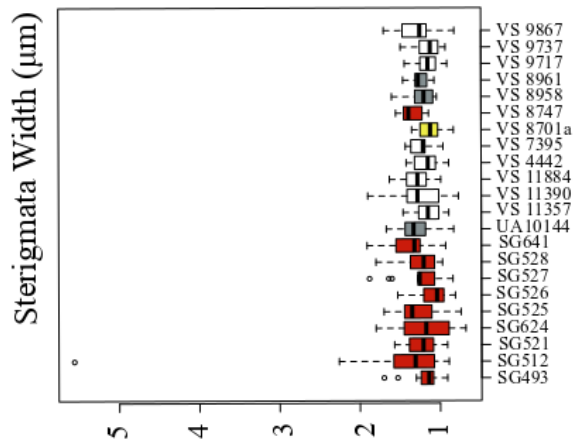
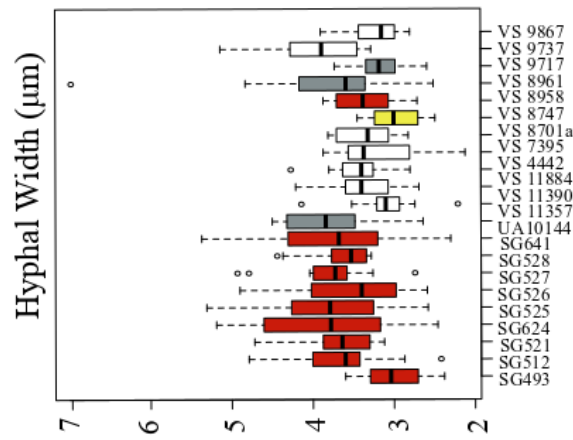


Figure 8 Box and whisker plot of each measurement by clade. Tukey HSD differences indicated by letters above. Basidium width, basidium length, basidiospore width, and sterigmata length were significantly different between *A. seborrheica* and all other species or groups. Basidiospore length was significantly different between Group II and all other species or groups.



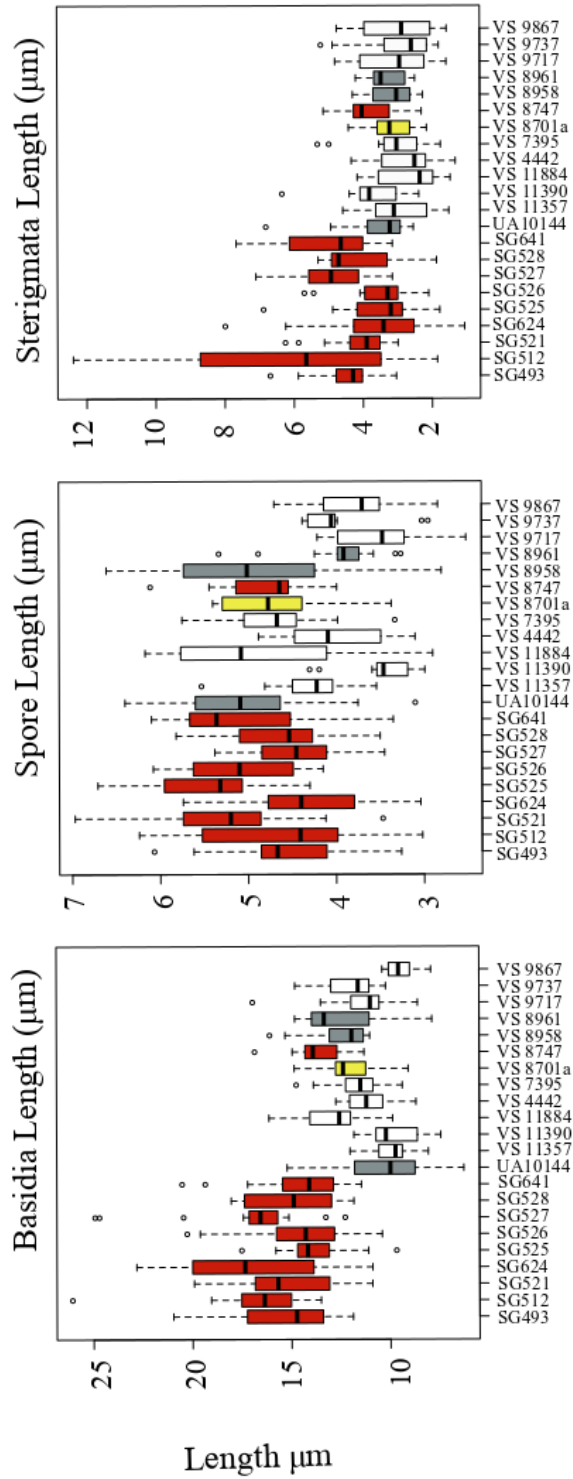


Figure 9 Box and whisker plot of all specimen measurements for a given morphological feature.

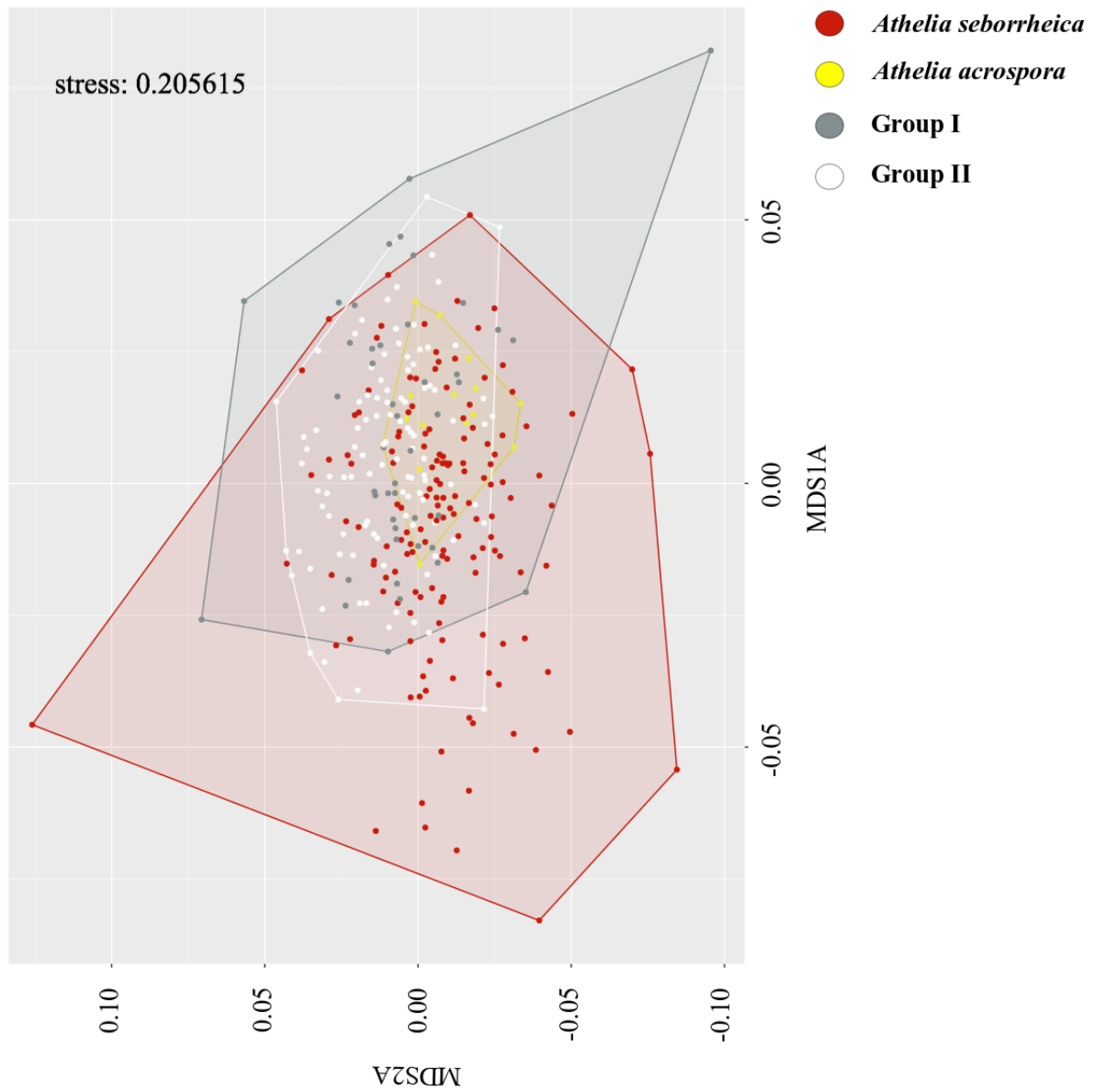
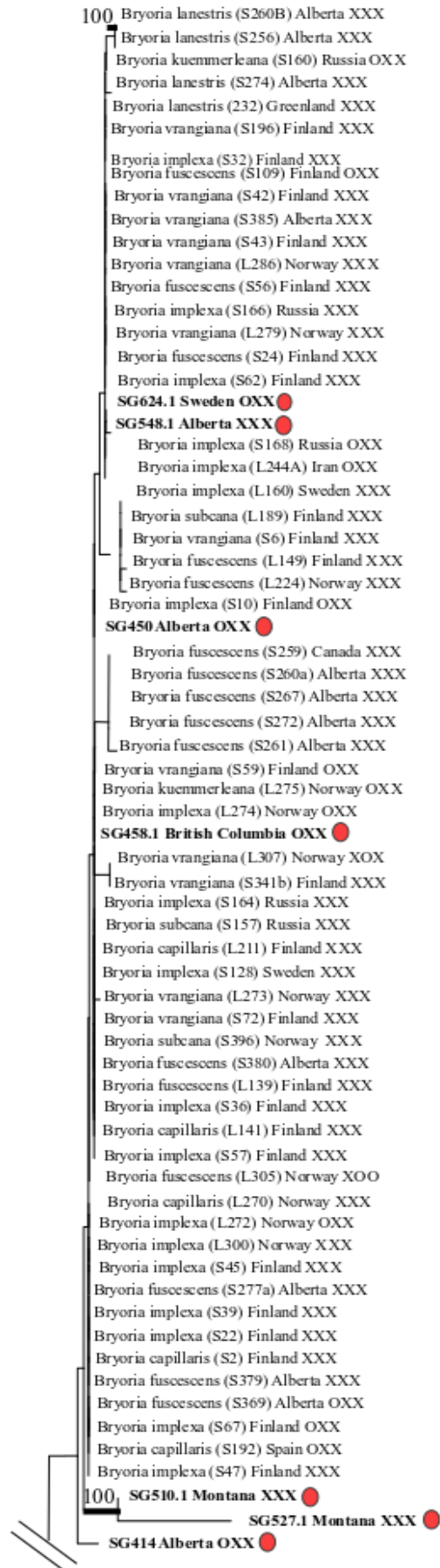


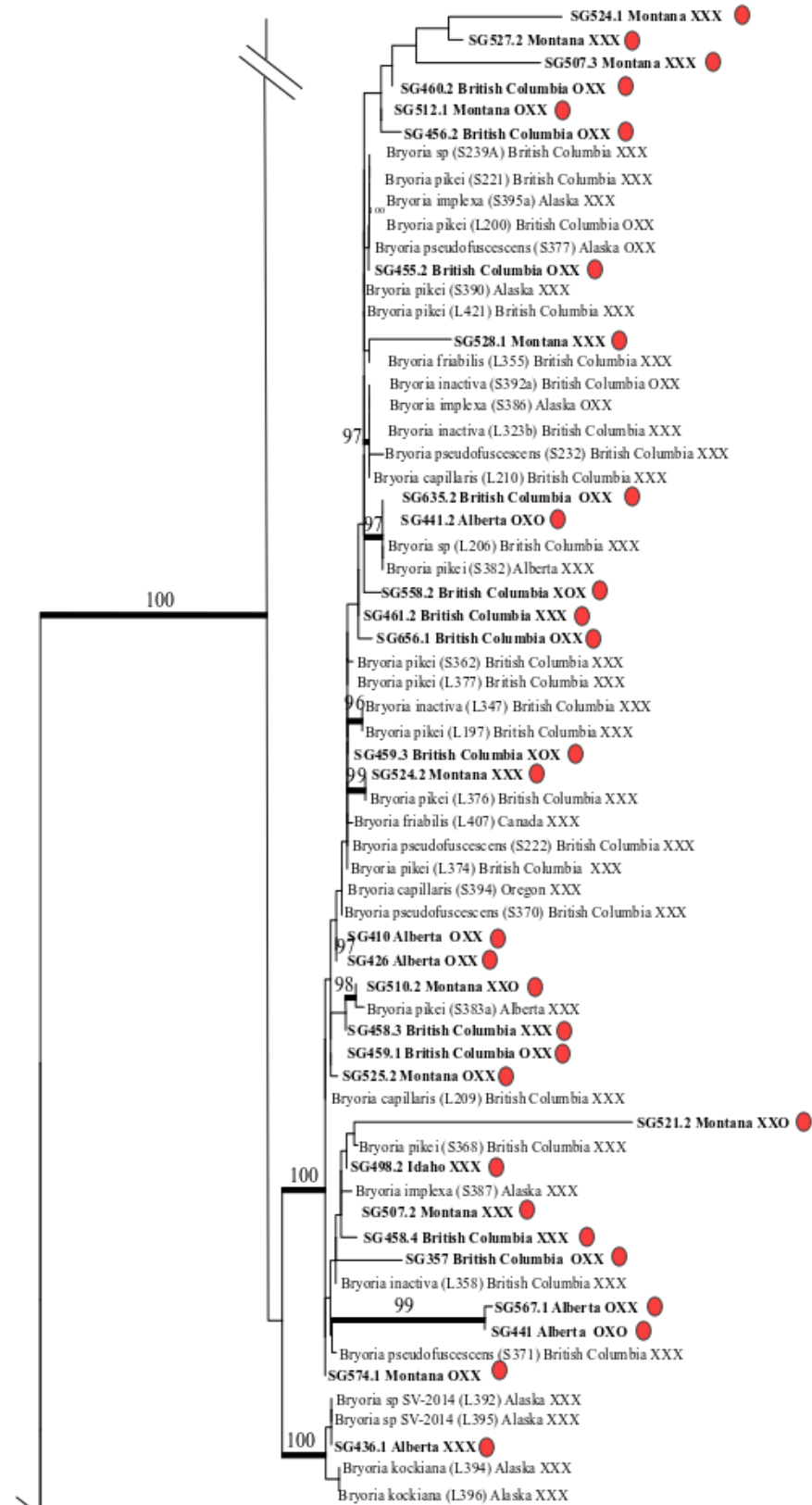
Figure 10 NMDS of *Athelia* morphological measurements calculated using "Euclidean" distances in two dimensions in the R package *vegan* (Oksanen et al., 2019). Hulls covering data points cover all points of a given species or grouping determined *a posteriori* to the generation of the concatenated tree in Fig. 2

ITS+ IGS + GAPDH, concatenated
 Number of characters: 2018
 469 variable sites
 118 parsimony informative sites

Partitioned ML

● *Athelia* infected





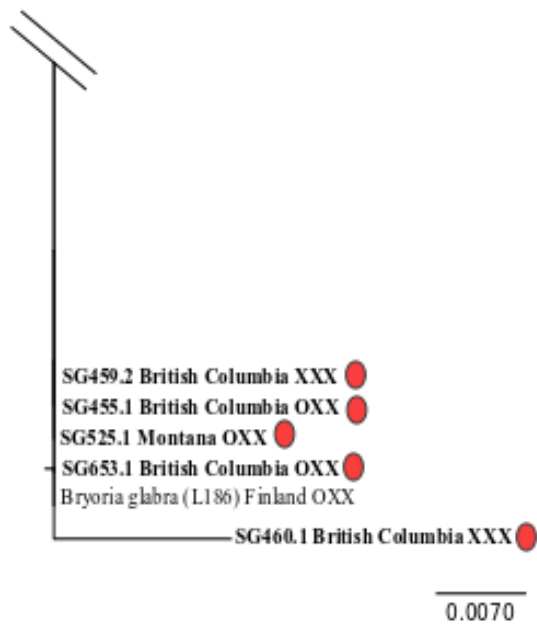


Figure 11 Concatenated ITS – IGS – GAPDH maximum likelihood Bryoria sect. Implexae tree. Branches with ultrafast bootstrapping support $\geq 95\%$ indicated with bolded bars. Bolded tip indicate sequences and specimens new to this study. X = a given locus was successfully sequenced or available on GenBank for a given specimen; O = a given locus was not successfully sequenced or available on GenBank for a given specimen. SG refers to Spencer Goyette's isolate numbers.



Plate 1 Healthy *Bryoria sp.* Photo by Spencer Goyette.

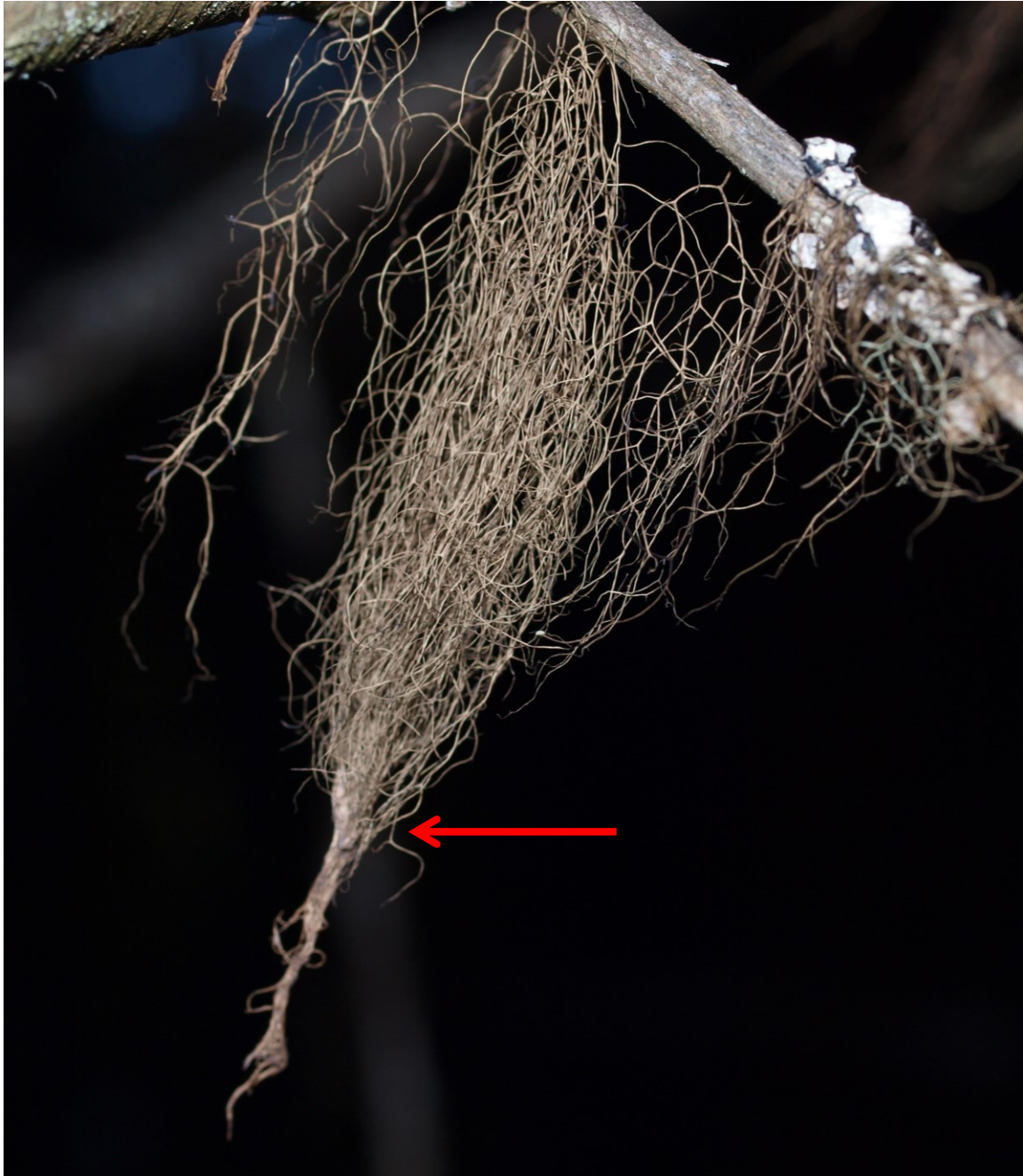


Plate 2 *Bryoria* sp. with rattail, indicated here with a red arrow. Photo by Spencer Goyette.



Plate 3 *Bryoria sp.* infected with an unknown fungal pathogen indicated here with red arrows. Note how the pattern of infection tracks the formation of rattails. Photo by Spencer Goyette.

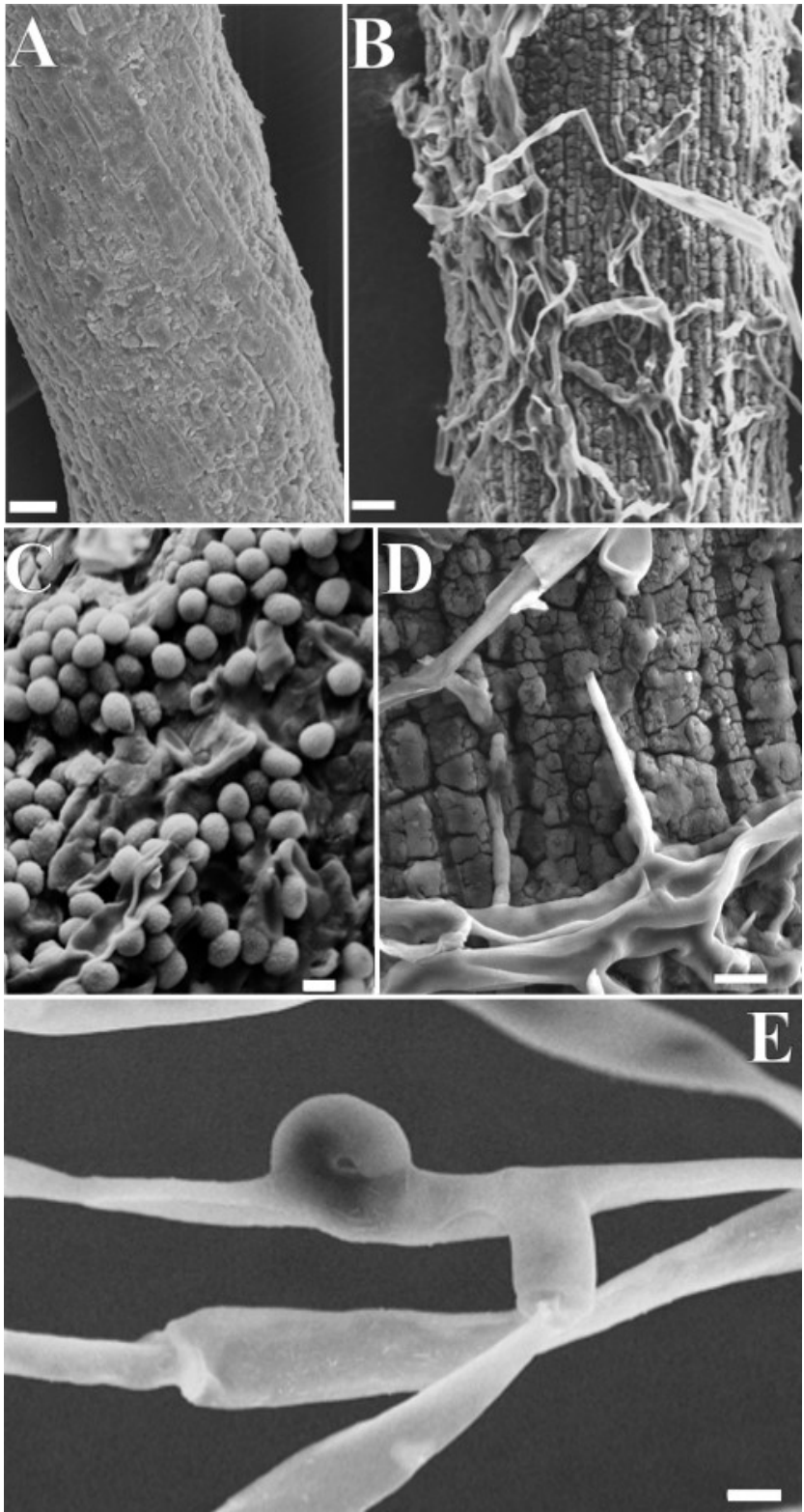


Plate 4 SEM micrographs taken on a Zeiss Sigma 300 VP-FESEM in the Department of Earth and Atmospheric Sciences at the University of Alberta.

A – Uninfected *Bryoria* thallus (scale bar 10 μm); **B** – *Bryoria* thallus infected with *Athelia seborrheica* (scale bar 10 μm); **C** – *Athelia seborrheica* basidiospores and basidia on *Bryoria* thallus (scale bar 2 μm); **D** – Close up of *Athelia seborrheica* on *Byoria* thallus (scale bar 2 μm); **E** – *Athelia seborrheica* clamp connection (scale bar 2 μm). Images by Spencer Goyette.



Plate 5 *Athelia* on lichen from a fallen *Larix* branch, emerging just after snowmelt outside Trego, Montana. Photo by Toby Spribille.

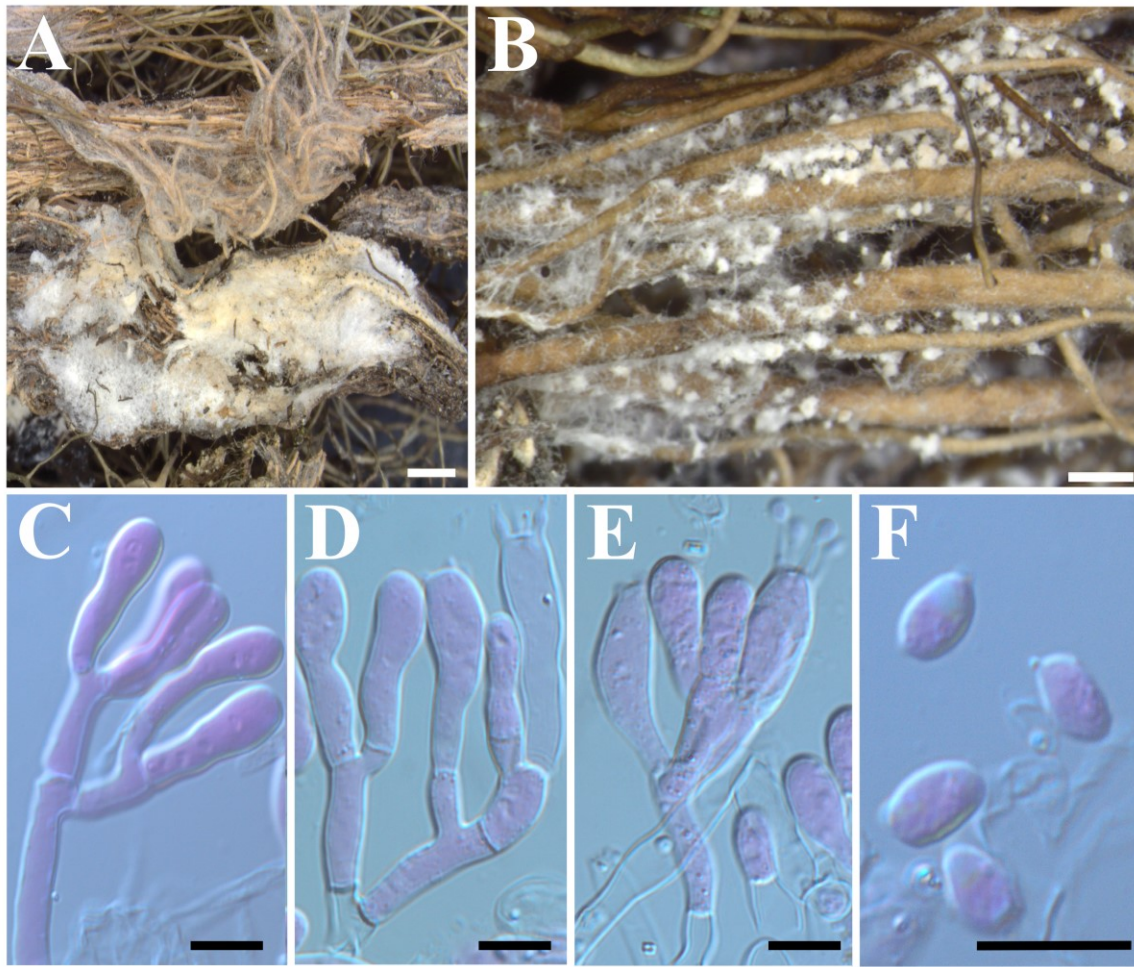


Plate 6 Basidiomata and sclerotia of *Athelia seborrheica*

A – basidioma on rattail (scale bar 1mm); **B** – sclerotia of *Athelia seborrheica* on rattailed *Bryoria* (scale bar 500µm); **C** – basidia (scale bar 10 µm); **D** – basidia with sterigmata (scale bar 10 µm); **E** – mature basidia with developing basidiospores attached to tips of sterigmata (10 µm); **F** – basidiospores (scale bar 10 µm). All squashes stained with 1% Phloxine-B in 5% potassium hydroxide.

REFERENCES

1. Adams, G.C. & Kropp, B.R. (1996). *Athelia arachnoidea*, the sexual state of *Rhizoctonia carotae*, a pathogen of carrot in cold storage. *Mycologia*, 88(3), 459-472.
2. Ahmadjian, V. (1993). *The Lichen Symbiosis*. John Willey and Sons, Inc.
3. Altschul, S.F., Gish, W., Miller, W., Myers, E.W. & Lipman, D.J. (1990). Basic local alignment search tool. *Journal of Molecular Biology*, 215(3), 403-410
4. Archer F, Adams P, & Schneiders B (2016). strataG: An R package for manipulating, summarizing and analysing population genetic data. *Molecular Ecology Resources*. doi: 10.1111/1755-0998.12559, <https://github.com/ericarcher/strataG>.
5. Baminger, U., Subramaniam, S.S., Renganathan, W., & Haltrich, D. (2001). Purification and characterization of Cellobiose Dehydrogenase from the plant pathogen *Sclerotium (Athelia) rolfsii*. *Applied and Environmental Microbiology*, 67(4), 1766-1774.
6. Bokhorst, S. Asplund, J., Kardol, P., & Wardle, D.A. (2015). Lichen physiological traits and growth forms affect communities of associated invertebrates. *Ecology*, 96(9), 2394-2407.
7. Boluda, C.G., Rico, V.J., Divakar, P.K., Nadyeina, O., Myllys, L., McMullin, R.T., Zamora, J.C., Scheidegger, S., & Hawksworth, D.L. (2019). Evaluating methodologies for species delimitation: the mismatch between phenotypes and genotypes in lichenized fungi (*Bryoria* sect. *Implexae*, Parmeliaceae). *Persoonia*, 42, 75-100.

8. Boluda, C.G., Rico, V.J., Crespo, A., Divakar, P.K., & Hawksworth, D.L. (2015). Molecular sequence data from populations of *Bryoria fuscescens* s. lat. in the mountains of central Spain indicates a mismatch between haplotypes and chemotypes. *The Lichenologist*, 47, 279–286.
9. Brodo, I.M. & Hawksworth, D.L. (1977). *Alectoria* and allied genera in North America. *Opera Botanica Series*, 42, 1-164.
10. Campbell, J. & Coxson, D.S. (2001). Canopy microclimate and arboreal lichen loading in subalpine spruce-fir forest. *Canadian Journal of Biology*, 79(5), 537-555.
11. Coxson, D.S. & Curteanu, M. (2002). Decomposition of hair lichens (*Alectoria sarmentosa* and *Bryoria* spp.) under snowpack in montane forest, Cariboo Mountains, British Columbia. *The Lichenologist*, 34(5), 395-402.
12. Dávalos, L.M., Cirranello, A.L., Geisler, J.H., & Simmons, N.B. (2012). Understanding phylogenetic incongruence: lessons from phyllostomid bats. *Biological Reviews of the Cambridge Philosophical Society*, 87(4), 991-1024.
13. Diederich, P., Lawrey, J.D., & Ertz, D. (2018). The 2018 classification and checklist of lichenicolous fungi, with 2000 non-lichenized, obligately lichenicolous taxa. *The Bryologist*, 121(3), 340-425.
14. Edwards, R., Soos, J., & Ritcey, R. (1960). Quantitative observations on epidendric lichens used as food by caribou. *Ecology*, 41(3), 425-431.
15. Eriksson, J. & Ryvarde, L. (1973). *Aleurodiscus* – *Confertobasidium*. The Corticiaceae of North Europe 2: 60 - 286. *Fungiflora*, Oslo, Norway.

16. Fryday, A.M. & Prather, L.A. (2001). The lichen collection of Henry Imshaug at the Michigan State University Herbarium (MSC). *The Bryologist*, 104(3), 464-467.
17. Gardes, M. & Bruns, T.D. (1993). ITS primers with enhanced specificity for basidiomycetes-application to the identification of mycorrhizae and rusts. *Molecular Ecology*, 2, 113-118.
18. Gargas, A., DePriest, P. T., Grube, M., Tehler, A., & Taylor, J.W. (1992). Polymerase chain reaction (PCR) primers for amplifying and sequencing nuclear 18S rDNA from lichenized fungi. *Mycologia*, 84, 589-592.
19. Gauslaa, Y. (2014). Rain, dew, and humid air as drivers of morphology, function and spatial distribution in epiphytic lichens. *The Lichenologist*, 46(1), 1-16.
20. Gauslaa, Y. (2002). Die back of epiphytic lichens in SE Norway – can it be caused by high rainfall in late autumn? *Graphis Scripta*, 13, 33-35.
21. Gilbert, O.L. (1988). Studies on the destruction of *Lecanora conizaeoides* by the lichenicolous fungus *Athelia arachnoidea*. *The Lichenologist*, 20(2), 183-190.
22. Ginns, J. & Worrall, J.J. (1999). *Athelia sibirica* new to North America and a key to the species of *Athelia* in Alaska and the Yukon Territory. *Kew Bulletin*, 54(3), 771-776.
23. Goward, T. (2008). Readings on the Lichen Thallus I: Face in the Mirror. *Evansia*, 25, 23-25.
24. Goward, T. (2003). On the vertical zonation of hair lichens (*Bryoria*) in the canopies of high-elevation oldgrowth conifer forests. *Canadian Field-Naturalist*, 117(1), 39-43.

25. Goward, T. (1999). The lichens of British Columbia: Illustrated keys. Part 2 Fruticose species. *British Columbia Ministry of Forests Special Report 9*, 1-319.
26. Goward, T. (1998). Observations on the ecology of the lichen genus *Bryoria* in high elevation conifer forests. *Canadian Field-Naturalist*, 112(3), 496-501.
27. Goward, T., McCune, B., & Meidinger, D. (1994). The lichens of British Columbia: Illustrated keys. Part 1 – Foliose and squamulose species. *British Columbia Ministry of Forests Special Report Series 8*, 1-181.
28. Großwindhager, C., Sachslehner, A., Nidetzky, B., & Haltrich, D. (1999). Endo-indhagd-mannanase is efficiently produced by *Sclerotium (Athelia) rolfsii* under derepressed conditions. *Journal of Biotechnology*, 67(2-3), 189-203.
29. Hall, T.A. (1999). BioEdit: a user-friendly biological sequence alignment editor and analysis program for Windows 95/98/NT. *Nucleic Acids Symposium Series*, 41, 95-98.
30. Harlton, C.E., Lévesque, C.A., & Punja, Z.K. (1995). Genetic diversity in *Sclerotium (Athelia) rolfsii* and related species. *Molecular Plant Pathology*, 85(10), 1269-1281.
31. Hawksworth, D.L. (2003). The lichenicolous fungi of Great Britain and Ireland: an overview and annotated checklist. *The Lichenologist*, 35(3), 191-232.
32. Hawksworth, D.L. (1983). A key to the Lichen-Forming, Parasitic, Parasymbiotic and Saprophytic Fungi Occurring on Lichens in the British Isles. *The Lichenologist*, 15(1), 1-44.
33. Hawksworth, D.L. (1977). Taxonomic and biological observations on the genus *Lichenoconium* (Sphaeropsidales). *Persoonia*, 9(2), 159-198.

34. Hoang, D.T., Chernomor, O., von Haeseler, A., Minh, B.Q., & Vinh, L.S. (2018). UFBoot2: Improving the ultrafast bootstrap approximation. *Molecular Biology and Evolution*, 35(2), 518–522.
35. Hofstetter, V., Buyck, B., Eyssartier, G., Schnee, S., & Gindro, K. (2019). The unbearable lightness of sequence-based identification. *Fungal Diversity*, 96, 243–284.
36. Jeffries, P. & Young, T.W. K. (1994). *Interfungal parasitic relationships*. CAB International.
37. Johnson, C., Parker, K., Heard, D. (2000). Feeding site selection by woodland caribou in north-central British Columbia. *Rangifer*, 20(5), 158-172.
38. Jülich, W. & Stalpers, J.A. (1980). *The resupinate non-poroid Aphylophorales of the temperate northern hemisphere*. North-Holland Publishing Company.
39. Jülich, W. (1972). Monographie der Athelieae (Corticaceae, Basidiomycetes). *Willdenowia, Beihefte* 7, 1-283.
40. Katoh, K. & Standley, D.M. (2013). MAFFT Multiple Sequence Alignment Software Version 7: Improvements in Performance and Usability. *Molecular Biology and Evolution*, 30(4), 772-780.
41. Lanfear, R., Frandsen, P. B., Wright, A. M., Senfeld, T., & Calcott, B. (2016). PartitionFinder 2: New methods for selecting partitioned models of evolution for molecular and morphological phylogenetic analyses. *Molecular Biology and Evolution*, 34(3), 772-773. DOI: [dx.doi.org/10.1093/molbev/msw260](https://doi.org/10.1093/molbev/msw260).

42. Larsen, M.J., Jurgensen, M.F., & Harvey, A.E. (1981). *Athelia epiphylla* associated with colonization of subalpine fir foliage under psychrophilic conditions. *Mycologia*, 73(6), 1195-1202.
43. Larsson, A. (2014). AliView: a fast and lightweight alignment viewer and editor for large data sets. *Bioinformatics*, 30(22): 3276-3278.
44. Lawrey, J.D., Binder, M., Diederich, P., Molina, M.C., Sikaroodi, M., & Ertz, D. (2007). Phylogenetic Diversity of lichen-associated homobasidiomycetes. *Molecular Phylogenetics and Evolution*, 44(2), 778-789.
45. Lawrey, J.D. & Diederich P. (2003). Lichenicolous fungi: Interactions, evolution, and biodiversity. *The Bryologist*, 106(1), 80-120.
46. Maser, C., Maser, Z., Witt, J.W., & Hunt, G. (1986). The northern flying squirrel: A mycophagist in southwestern Oregon. *Canadian Journal of Zoology*, 64(10), 2086-2089.
47. Matsuura, K., Tanaka, C., & Nishida, T. (2000). Symbiosis of a termite and a sclerotium-forming fungus: Sclerotia mimic termite eggs. *Ecological Research*, 15, 405-414.
48. McCune, B. (2000). Lichen communities as indicators of forest health. *The Bryologist*, 103(2), 353-356.
49. Myllys, L., Velmala, S., Holien, H., Halonen, P., Wang, L.-S., & Goward, T. (2011). Phylogeny of the genus *Bryoria*. *The Lichenologist*, 43(6), 617-638.

50. Myllys, L., Stenroos, S., & Thell, A. (2002). New genes for phylogenetic studies of lichenized fungi: Glyceraldehyde-3-phosphate dehydrogenase and beta-tubulin Genes. *The Lichenologist*, 34(3), 237-246.
51. Nei, M., & Kumar, S. (2000). *Molecular Evolution and Phylogenetics*. Oxford University Press, Oxford.
52. Nguyen, L.-T., Schmidt, H.A., von Haeseler, A., & Minh, B.Q. (2015). IQ-TREE: A fast and effective stochastic algorithm for estimating maximum likelihood phylogenies. *Molecular Biology and Evolution*, 32(1), 268-274.
53. Okabe, I. & Matsumoto, N. (2003). Phylogenetic relationship of *Sclerotium rolfsii* (teleomorph *Athelia rolfsii*) and *S. delphinii* based on ITS sequences. *Mycological Research*, 107(2), 164-168.
54. Oksanen, J., Blanchet, F.G., Friendly, M., Kindt, R., Legendre, P., McGlinn, D., Minchin, P.R., O'Hara, R.B., Simpson, G.L., Solymos, P., Stevens, M.H.H., Szoecs, E., & Wagner, H. (2019). vegan: Community Ecology Package. *R package version 2.5-6*. <https://CRAN.R-project.org/package=vegan>
55. Orange, A., James, P.W., & White, F.J. (2001). *Microchemical methods for the identification of lichens*. British Lichen Society.
56. Paradis, E. (2010). pegas: an R package for population genetics with an integrated–modular approach. *Bioinformatics*, 26, 419-420
57. Pettersson, R.B., Ball, J.P., Renhorn, K.-E., Esseen, P.-A., & Sjöberg, K. (1995). Invertebrate communities in boreal forest canopies as influenced by forestry and lichens with implications for passerine birds. *Biological Conservation*, 74(1), 57-63.

58. Petrini, O., Hake, U., & Dreyfus M. (1990). An analysis of fungal communities isolated from fruticose lichens. *Mycologia*, 82(4), 444-451.
59. Pike, L.H. (1978). The importance of epiphytic lichens in mineral cycling. *The Bryologist*, 81(2), 247-257.
60. Printzen, C. & Ekman, S. (2002). Genetic variability and its geographical distribution in the widely disjunct *Cavernularia hulthenii*. *The Lichenologist*, 34(2), 101-111.
61. QGIS.org (2.18). QGIS Geographic Information System. Open Source Geospatial Foundation Project. <http://qgis.org>
62. R Core Team. (2019). R: A language and environment for statistical computing. *R Foundation for Statistical Computing, Vienna, Austria*. URL <https://www.R-project.org/>.
63. Rambaut, A. (2014). FigTree v1.4.2. Available at: <http://tree.bio.ed.ac.uk/software/figtree/>
64. Rambold, G. & Triebel, D. (1992). The inter-Lecanoralean associations. *Bibliotheca Lichenologica, Band 48*, 1-201.
65. Rehner, S.A. & Buckley, E. (2005). A *Beauveria* phylogeny inferred from nuclear ITS and EF1- α sequences: evidence for cryptic diversification and links to *Cordyceps* teleomorphs. *Mycologia*, 97(1), 84-98.
66. Resl, P. (2015). phylo-scripts: Python scripts for phylogenetics. release v0.1. available at: <http://github.com/reslp>
67. Resl, P., Schneider, K., Westberg, M., Printzen, C., Palice, Z., Thor, G., Fryday, A., Mayrhofer, H., & Spribille, T. (2015). Diagnostics for a troubled backbone: testing

topological hypotheses of trapelioid lichenized fungi in a large-scale phylogeny of Ostropomycetidae (Lecanoromycetes). *Fungal Diversity*, 73, 239-258.

68. Roger, A., Sandblom, O., Doolittle, W., & Philippe, H. (1999). An evaluation of elongation factor 1 alpha as a phylogenetic marker for eukaryotes. *Molecular Biology and Evolution*, 16(2), 218-233.
69. Rominger, E., Robbins, C., & Evans, M. (1996). Winter foraging ecology of woodland caribou in northeastern Washington. *The Journal of Wildlife Management*, 60(4), 719-728.
70. Rosenthal, L., Larsson, K.-H., Branco, S., Chung, J., Glassman, S., Liao, H., Peay, K., Smith, D., Talbot, J., Taylor, J., Vellinga, E., Vilgalys, R., & Bruns, T. (2017). Survey of corticioid fungi in North American pinaceous forests reveals hyperdiversity, underpopulated sequence databases, and species that are potentially ectomycorrhizal. *Mycologia*, 109(1), 115-127.
71. Schoch, C., Seifert, K., Huhndorf, S., Robert, V., Spouge, J., Levesque, C., Chen, W., & Fungal Barcoding Consortium. (2012). Nuclear ribosomal transcribed spacer (ITS) region as a universal DNA barcode marker for Fungi. *Proceedings of the National Academy of Sciences of the United States of America*, 109(16), 6241-6246.
72. Shimodaira, H. (2002). An Approximately Unbiased Test of Phylogenetic Tree Selection. *Systematic Biology*, 51(3), 492-508.
73. Spribille, T., Taghirdzhanova, G., Goyette, S., Tuovinen, V., Case, R., & Zandberg, W.F. (2020). 3D biofilms: in search of the polysaccharides holding together lichen symbioses. *FEMS Microbiology Letters*, 367(5), fnaa023. DOI: 10.1093/femsle/fnaa023.

74. Spribille, T. (2018). Relative symbiont input and the lichen symbiotic outcome. *Current Opinion in Plant Biology*, 44, 57-63.
75. Spribille, T., Tuovinen, V., Resl, P., Vanderpool, D., Wolinski, H., Aime, M.C., Schneider, K., Stabentheiner, E., Toome-Heller, M., Thor, G., Mayrhofer, H., Johannesson, H., & McCutcheon, J.P. (2016). Basidiomycete yeasts in the cortex of ascomycete macrolichens. *Science*, 353(6298), 488-492.
76. Stubbs, C. (1989). Patterns of distribution and abundance of corticolous Lichens and their invertebrate associates on *Quercus rubra* in Maine. *The Bryologist*, 92(4), 453-460.
77. Thomas, D., Edmonds, E., & Brown, W. (1996). The diet of woodland caribou populations in west-central Alberta. *Rangifer: Special Issue*, 9, 337-342.
78. Tuovinen, V., Ekman, S., Thor, G., Vanderpool, D., Spribille, T., & Johannesson, H. (2019). Two basidiomycete fungi in the cortex of wolf lichens. *Current Biology*, 29(4), 476-483.e5.
79. Velmala, S., Myllys, L., Goward, T., Holien, H., & Halonen, P. (2014). Taxonomy of *Bryoria* section *Implexae* (Parmeliaceae, Lecanoromycetes) in North America and Europe, based on chemical, morphological and molecular Data. *Annales Botanici Fennici*, 51(6), 345-371.
80. Ward, R.L. & Marcum, C.L. (2010). Lichen litterfall consumption by wintering deer and elk in western Montana. *The Journal of Wildlife Management*, 69(3), 1081-1089.
81. White, T. J., Bruns, T.D., Lee, S.B., & Taylor, J.W. (1990). Amplification and direct sequencing of fungal ribosomal RNA genes for phylogenetics. Pp. 315–321. In:

PCR protocol: A guide to methods and applications. Eds., M. Innis, A., Gelfand, D.H., Sninsky, J.J., & White, T.J. Academic Press, New York.

82. Xu, Z., Harrington, T.C., Gleason, M.L., & Batzer, J.C. (2010). Phylogenetic placement of plant pathogenic *Sclerotium* species among teleomorph genera. *Mycologia*, 102(2), 337-346.
83. Yurchenko, E.O. & Golubkov, V.V. (2003). The morphology, biology, and geography of a necrotrophic basidiomycete *Athelia arachnoidea* in Belarus. *Mycological Progress*, 2(4), 275-284.